UC Santa Cruz
UC Santa Cruz Previously Published Works

Title

Vertical Distribution of Rocky Intertidal Organisms Shifts With Sea-Level Variability on the Northeast Pacific Coast.

Permalink

Journal

ISSN

Authors

Kaplanis, Nikolas J
Denny, Mark W
Raimondi, Peter T

Publication Date

DOI

Copyright Information

Peer reviewed

RESEARCH ARTICLE OPEN ACCESS

Vertical Distribution of Rocky Intertidal Organisms Shifts With Sea-Level Variability on the Northeast Pacific Coast

Nikolas J. Kaplanis[1] 🄳 | Mark W. Denny[2] | Peter T. Raimondi[1]

[1]Department of Ecology and Evolutionary Biology, University of California, Santa Cruz, Santa Cruz, California, USA | [2]Hopkins Marine Station of Stanford University, Pacific Grove, California, USA

Correspondence: Nikolas J. Kaplanis (nkaplanis@ucsc.edu)

ABSTRACT

Disentangling the effects of cyclical variability in environmental forcing and long-term climate change on natural communities is a major challenge for ecologists, managers, and policy makers across ecosystems. Here we examined whether the vertical distribution of rocky intertidal taxa has shifted with sea-level variability occurring at multiple temporal scales and/or long-term anthropogenic sea-level rise (SLR). Because of the distinct zonation characteristic of intertidal communities, any shift in tidal dynamics or average sea level is expected to have large impacts on community structure and function. We found that across the Northeast Pacific Coast (NPC), sea level exhibits cyclical seasonal variability, tidal amplitude exhibits ecologically significant variability coherent with the 18.6-year periodicity of lunar declination, and long-term sea-level rise is occurring. Intertidal taxa largely do not exhibit significant vertical distribution shifts coherent with short-term (monthly to annual) sea-level variability but do exhibit taxa-specific vertical distribution shifts coherent with cyclical changes in lunar declination and long-term SLR at decadal timescales. Finally, our results show that responses to cyclical celestial mechanics and SLR vary among taxa, primarily according to their vertical distribution. Long-term SLR is occurring on ecologically relevant scales, but the confounding effects of cyclical celestial mechanics make interpreting shifts in zonation or community structure challenging. Such cyclical dynamics alternatingly amplify and dampen long-term SLR impacts and may modify the impacts of other global change related stressors, such as extreme heat waves and swell events, on intertidal organisms living at the edge of their physiological tolerances. As a result, intertidal communities will likely experience cyclical periods of environmental stress and concomitant nonlinear shifts in structure and function as long-term climate change continues. Our results demonstrate that consistent, large-scale monitoring of marine ecosystems is critical for understanding natural variability in communities and documenting long-term change.

1 | Introduction

The rocky intertidal zone is a model system for exploring interactions between ecology and the physical environment, in part because it is characterized by patterns of ecological zonation in the form of distinct banding along the tidal elevation gradient. Intertidal community zonation has classically been identified as driven by spatially and density-dependent ecological mechanisms including competition (Connell 1961; Menge 1976), mutualism (Menge 1995), predation (Menge 1976; Paine 1969, 1974, 1980), facilitation (Johnson and Brawley 1998; Readdie 2004), and larval supply (Gaines and Roughgarden 1985; Johnson and Brawley 1998; Roughgarden, Gaines, and Possingham 1988) and physical drivers such as waves, tides, and nearshore currents (Connell 1961, 1972; Dayton 1971; Doty 1946; Harley, Helmuth, and Carolina 2003; Lewis 1964; Paine 1974). Generally, according to Connell's rule, in the intertidal zone the lower limits of distribution are set by biotic factors, and the upper limits are set by abiotic factors, namely desiccation rates determined by average sea-level conditions (Connell 1961). Sea level varies on multiple spatiotemporal scales that each may have significant consequences for the structure of rocky intertidal ecosystems through modifying physical environmental conditions, including emersion time and desiccation stress (Figure 1; Table 1; Chelton and Davis 1982; Stommel 1963). Despite this, both sea-level and vertical distribution (the observed occupancy by intertidal organisms of distinct elevations in reference to any fixed point at a field site) are largely assumed to be temporally stable in ecological studies (Readdie 2004). This is at least partly a result of the short time frames over which data are typically collected in experimental and observational studies relative to the time frames over which physical drivers of vertical distribution vary. Experimental manipulations of ecological players, such as Paine's removal of the keystone predator *Pisaster ochraceous* (Brandt 1835), can induce rapid, observable changes in vertical distribution (Paine 1974). In contrast, changes in physical environmental conditions that are consequential for patterns of vertical distribution are challenging to simulate experimentally and naturally occur over time scales that are not amenable to observational studies (i.e., multi-annual to multi-decadal scales; Figure 1; Table 1).

To date, few studies have examined the effects of sea-level variability on intertidal vertical distribution because the inherent complexity and spatial and temporal scale of sea-level variability pose substantial logistical challenges to identifying its ecological impacts (Denny and Paine 1998). To detect ecological responses to sea-level variability and fully understand community dynamics, it is necessary to pair long-term and large-scale physical and ecological datasets (Denny and Paine 1998). But these datasets must have certain characteristics. Tide gauges that produce sea-level time series must record conditions near the open coast within a reasonable proximity of locations where ecological monitoring occurs. Ecological monitoring must be spatially explicit and capable of providing vertical distribution data in association with species identifications. Ecological data must also be geographically and temporally resolved and at least multi-decadal in temporal extent to capture the major fluctuations in
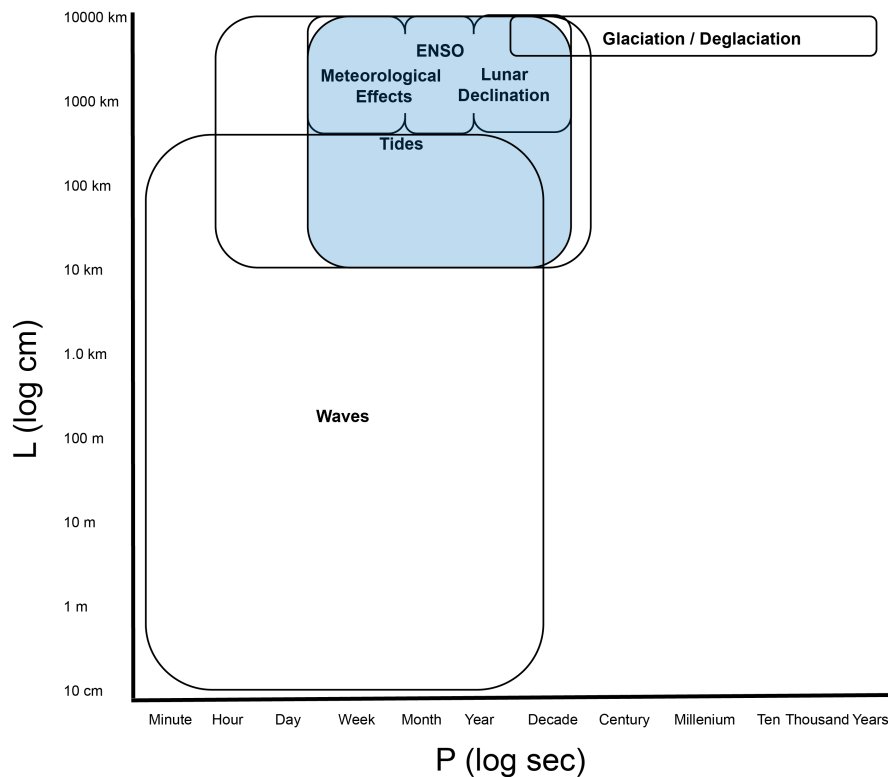
FIGURE 1 | Schematic diagram of approximate scale of spatiotemporal drivers of sea-level variability experienced in the rocky intertidal zone (adapted from Stommel 1963). On the *x*-axis is the logarithm of the temporal scale P, in seconds, and on the *y*-axis is the logarithm of the spatial scale L, in centimeters, over which variation in these drivers have effects on rocky intertidal organisms. The approximate scales of variation examined in this paper are highlighted in blue.

TABLE 1 | Scales of sea-level variability and their impact on the vertical distribution of rocky intertidal taxa. The table shows known drivers of sea-level variability and their impact on vertical distribution from the literature. Drivers at scales examined by this paper are shaded in gray.

Sea level	Driver	Temporal scale	Spatial scale	Magnitude of effect	Mechanism of change/ major findings	Citations
Isostatic	Waves	minutes–years	m to hundreds of km		Wave runup raises upper limit by decreasing desiccation	Lewis 1964; Harley, Helmuth, and Carolina 2003
	Tides	hours–decades	tens–thousands of km			Lewis 1964, 1978
	Meteorological seasonal effects	days–months	hundreds–thousands of km			
	ENSO oscillation	months–years	hundreds–thousands of km	tens of cm	No significant effect	Menge, Chan, and Lubchenco 2008
	Lunar declination	4.4–18.6 years	hundreds–thousands of km	tens of cm	Change in emergence times, shift in vertical zonation (10's of cm)	Denny and Paine 1998; Readdie 2004; Hunt 2006; Harley and Paine 2009; Burnaford, Nielsen, and Williams 2014
Eustatic	Anthropogenic sea-level rise	decades to thousands of years	tens of thousands of km	tens of m	Coastal squeeze leading to habitat loss	Vaselli et al. 2008; Jackson and McIlvenny 2011; Thorner, Kumar, and Smith 2014; Kaplanis et al. 2020
	Glaciation/deglaciation	decades to thousands of years	tens of thousands of km	hundreds of m	Habitat loss, change in relative proportion of sandy to rocky shoreline, changes to connectivity and biogeography	Valentine and Jablonski 1991; Graham et al. 2003; Toms et al. 2014

tidal conditions driven by long-term celestial mechanics (Denny and Paine 1998; Haigh, Eliot, and Pattiaratchi 2011; Menéndez and Woodworth 2010). Data matching all these criteria are rare.

The few studies that have documented changes in vertical distribution of intertidal organisms linked to causal mechanisms at different temporal scales suggest that the paradigm of spatial heterogeneity, but temporal stability, deserves further scrutiny. Seasonal shifts in foliose algae, upward in the spring, then back down again as production decreases, have been documented in Australia (Underwood 1980; Underwood and Jernakoff 1984). At Tatoosh Island, Washington, USA, Denny and Paine (1998) documented a long-term (1971–1988) downward shift of ~0.20 m in the upper limit of *Mytilus californianus* Conrad, 1837 that was proposed to be driven by 18.6-year periodicity fluctuation in tidal exposure linked to oscillation in the plane of the moon's orbit (lunar declination) (Denny and Paine 1998). Also at Tatoosh Island, Harley and Paine (2009) found that over 30 years, the upper limit of *Mazzaella parksii* (Setchell & N.L. Gardner) Hughey, P.C. Silva & Hommersand 2001 did not track gradual changes in air temperature and dropping relative sea level associated with continental uplift, but rather exhibited consistent seasonal fluctuations of approximately 3.0 cm upward in the winter and downward in the summer, and two large downward displacements of approximately 0.10–0.20 m during two summers (1995, 2004) associated with unusually calm wave conditions combined with unusually warm air temperatures (Harley and Paine 2009). Using data at eight long-term monitoring (LTM) sites in south central California, Readdie (2004) documented significant (+ 0.06–0.63 m) shifts in the upper limits of the *Chthamalus/Balanus*, *Endocladia*, and *Silvetia* zones over the course of a decade (1992–2002), attributed to facilitated ecological succession (Readdie 2004). Although they did not explicitly document shifts in distribution, Burnaford, Nielsen, and Williams (2014) documented a change in percent cover of the canopy forming intertidal kelp *Saccharina sessilis* (C. Agardh) Kuntze 1891 over 14 years (1998–2012) in fixed plots at San Juan Island, WA, USA, in response to changes in emersion time associated with the lunar declination cycle (Burnaford, Nielsen, and Williams 2014). This could have represented a change in abundance of *S. sessilis* at that site, or potentially a shift in the distribution of the algae to a different elevation. Together, these results suggest that both cyclical and punctuated, stochastic shifts in vertical distribution of 10's of cm over seasonal to multi-decadal timescales may be an important characteristic of intertidal ecosystems and their ecological dynamics. As a result, any attempt to examine the effects of long-term climatic trends on intertidal communities, such as anthropogenic sea-level rise (SLR), must consider both cyclical and stochastic variation in physical drivers of community structure at multiple (i.e., multi-annual to multi-decadal) time scales.

Anthropogenic warming of the atmosphere and oceans and resultant deglaciation is causing sea-level rise (Cazenave et al. 2014; Chen et al. 2017; Church and White 2006; National Research Council 2012; Rahmstorf 2010; Sweet et al. 2017). Unlike the cyclical rise and fall in the vertical distribution of intertidal organisms documented in the past, SLR is hypothesized to drive a long-term nonlinear upward shift in the vertical distribution of intertidal organisms through time. Although estimates remain uncertain, some studies project up to 2.5 m of SLR on the NPC by 2100 (Church and White 2006; Sweet et al. 2017). This large-magnitude

SLR is expected to have drastic ecological impacts on rocky shores on the NPC, because it is expected to lead to an upward shift in the vertical distribution of intertidal organisms (Figure 2). Yet studies documenting long-term shifts in zonation associated with SLR are almost entirely lacking. Using historical photographs at the Hopkins Marine Station in Pacific Grove, CA, USA, Hunt (2006) documented an upward shift in the upper limits of *Endocladia muricata* (Endlicher) J. Agardh, 1847 of comparable magnitude to rising sea level over the course of a century (1896–2006), but occurring in a single large step from 1963 to 1970, and attributed to intraspecific facilitation (Hunt 2006). Studies modeling the future impacts of SLR on intertidal communities suggest that when backed by steep cliffs, large-magnitude SLR associated upward shifts will result in coastal squeeze as the total surface area associated with any tidal elevation range is reduced, ultimately leading to substantial habitat loss, intensified competition, and declines in populations of intertidal taxa (Hollenbeck, Olsen, and Haig 2014; Jackson and Mcilvenny 2011; Kaplanis et al. 2020; Schaefer et al. 2020; Thorner, Kumar, and Smith 2014). Addressing the question of how rocky intertidal communities have responded to SLR in the past is valuable, as past periods of elevated sea level may serve as a proxy for future conditions and the resultant community response.

The Northeast Pacific Coast (NPC) is an ideal study location for examining the effects of SLR on vertical distribution of intertidal organisms because of its long history of monitoring of both sea-level and rocky intertidal biota. The National Oceanic and Atmospheric Administration Center for Operational Oceanographic Products and Services (NOAA CO-OPS) manages a network of over 75 tide gauge stations across the West Coast that provide detailed sea-level data, with some time series starting in the 1800s (Figure 3). These time series have both a short sampling interval (high resolution) and long temporal extent and thus allow characterization of sea-level variability from hourly to multi-decadal scales. The Multi-Agency Rocky Intertidal Network (MARINe) has monitored rocky intertidal communities at sites across the NPC for over two decades. This program provides detailed, spatially explicit community composition data at nearly 200 rocky intertidal field sites from Baja California, México, to Alaska, United States (Figure 3). The MARINe Coastal Biodiversity Survey (CBS) has been carried out since 2001, spanning a complete 18.6-year lunar declination cycle and its associated variability in tidal amplitude, as well as two decades of long-term SLR. The pairing of these datasets provides a unique opportunity to examine sea-level variability and its consequences for rocky intertidal organisms at scales commensurate with those at which variability occurs.

The purpose of this study was to (1) characterize spatiotemporal sea-level variability on rocky shores of the NPC and (2) determine the relationship between this sea-level variability and the distribution of rocky intertidal organisms over the past two decades. Specifically, we asked the questions: (1) What are the seasonality and long-term trends in sea level across the NPC and through the long-term monitoring period? (2) Does the vertical distribution of rocky intertidal organisms shift coherently with sea-level variability? To address Question 1, we characterized seasonality and long-term trends for tide gauge stations in eight regions across the NPC, from Southern California to Southeast Alaska. To address Question 2, we evaluated whether the upper limits of vertical
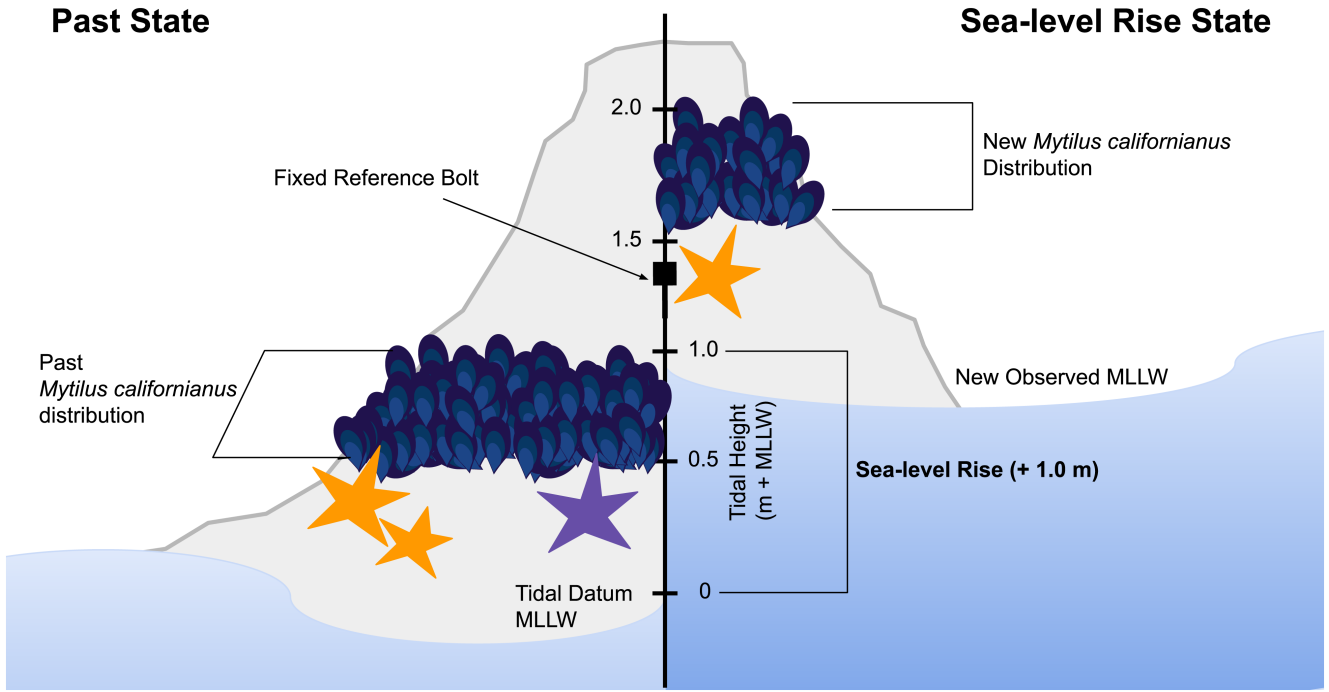
FIGURE 2 | Schematic diagram of change in vertical distribution of intertidal organisms under SLR. As sea-level rises, zonation patterns remain constant in reference to the actual observed average sea-level conditions experienced at the site (observed mean lower low water, MLLW), but intertidal organisms exhibit an upward shift in reference to both the fixed, antiquated tidal datum (tidal datum MLLW), and to any fixed point on the shore. In this theoretical example, *Mytilus californianus* occupies 0.5 vertical m in both states with an upper limit 1.0 m above sea level but shifts from a range of 0.5–1.0 m + Datum MLLW to a new range of 1.5–2.0 m + Datum MLLW under the influence of 1.0 m of sea-level rise. The *Mytilus californianus* distribution is also observed to move from below to above a fixed reference bolt, like those found at MARINe CBS sites. If the magnitude of sea-level rise is sufficiently large, and the slope at the heights occupied is steeper than in the past, then organisms experience a loss of habitat availability, termed "coastal squeeze."
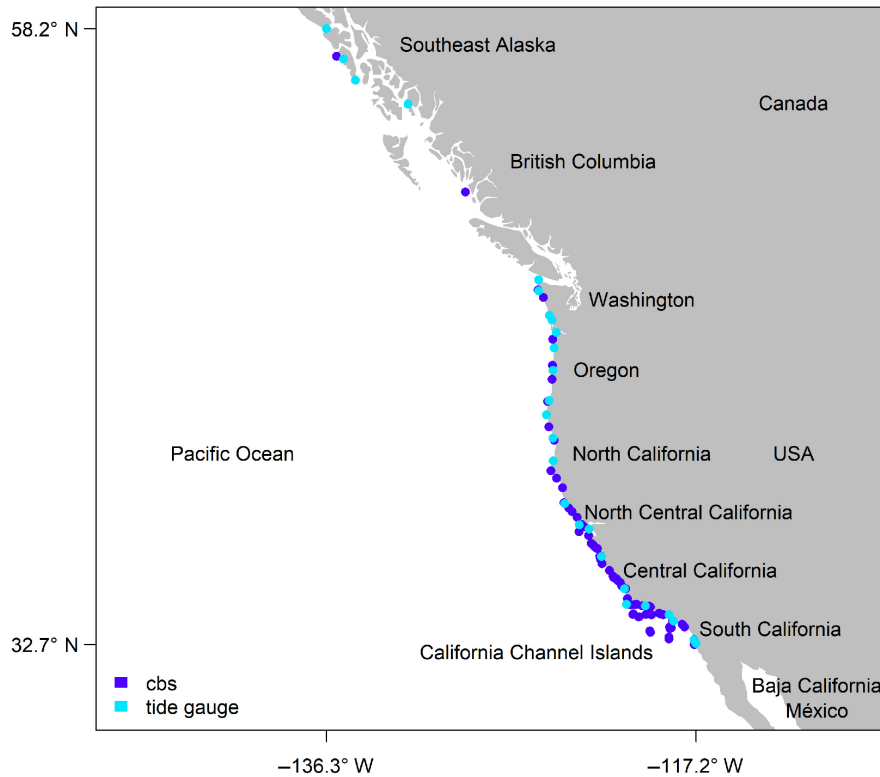
FIGURE 3 | Study map of the Northeast Pacific Coast. Locations of 26 National Oceanic and Atmospheric Administration (NOAA) tide gauge stations (light blue) and Multi-Agency Rocky Intertidal Network (MARINe) Coastal Biodiversity Survey (CBS) sites (dark blue) shown. Study region names are written.

distribution of dominant benthic intertidal taxa at 77 MARINe CBS sites has shifted coherently with sea-level variability across a range of temporal scales. We hypothesized that intertidal taxa would exhibit shifts in vertical distribution in response to the long-term (multi-decadal) sea-level trends (S) at stations nearest the CBS survey sites. We expected this response to be spatially variable but that most taxa would exhibit upward shifts in vertical distribution as sea-level rises, on the order of a few cm. We expected that lunar declination (ld) would have different effects on intertidal taxa depending on their vertical distribution and the respective influence of the components of the tidal cycle and overall tidal amplitude (Greater Diurnal Range, gt) modified by variability in lunar declination (*sensu* Denny and Paine 1998; Menéndez and Woodworth 2010; Haigh, Eliot, and Pattiaratchi 2011). We hypothesized that upper intertidal taxa would have a positive correlation with lunar declination, shifting upward as mean higher high water (MHHW) and gt increase toward the lunar declination maxima. Conversely, we hypothesized that taxa occurring at low to intermediate tidal heights (below approximately mean lower high water (MLHW)) would shift upward toward the lunar declination minima, when the MLHW values are elevated, causing a second period of tidal submersion or wetting in each day. We hypothesized that whether this effect dampens or amplifies the sea-level rise effect would depend on whether the cycle is in or out of synch with SLR during the CBS surveys. We expected the magnitude of the ld effect would be similar to that of the long-term sea-level trend, but that it would be spatially variable, decreasing with increasing latitude (*sensu* Haigh, Eliot, and Pattiaratchi 2011). Finally, we expected that the long-term responses would be modified by shorter term sea-level variability (monthly deviations (d), preceding annual minimum (L) and maximum (M) deviations, and preceding year annual mean of deviations (đ) from the long-term trend (S)). We expected that life history differences across taxa would determine to some extent the strength of the relationships with these predictor variables, with shorter lived taxa (e.g., *Balanus glandula* Darwin, 1854, opportunistic algae) responding more readily to short-term variability. We expected geographic location (latitude (y) and longitude (x)) would modify the relationships due to differences in various site characteristics, including site geomorphology (e.g., habitat availability, slope, and aspect), environmental conditions (e.g., wave exposure, air and water temperatures), and the interactions between these characteristics. Generally, we hypothesized that upper limits would increase upcoast toward the northwest, due to increases in wave exposure, cooler air temperatures, and generally damper air conditions.

2 | Materials and Methods

2.1 | Characterizing Sea-Level Variability— Seasonality and Long-Term Trends

We analyzed verified monthly mean sea-level (MMSL) values calculated from hourly tidal-height readings each month at 26 NOAA CO-OPS tide gauge stations within eight regions in the NPC from Southeast Alaska to Southern California (Figure 3). MMSL values are referenced to mean lower low water (MLLW) at each station, the arithmetic mean of all lower low water tidal heights observed over the National Tidal Datum Epoch (NTDE) from 1983 to 2001 (NOAA 2001). MMSL data from these stations were constrained to the 2001/01–2022/09 period

(261 months, or 21.75 years) to match the temporal extent of the MARINe CBS data available up to the time of analysis. Only stations with a data extent of at least 15 years and that are located on or near the open coast were used. To visualize sea-level data, we created time-plots of the series at each station (e.g., Figure 4). To visualize fluctuations driven by lunar declination, a sinusoidal function with a period of 18.61 years was fitted to the monthly great diurnal range (gt) values for each tide gauge station using ordinary least squares regression (Figure 5).

To understand seasonality, we first used autocorrelation function (ACF) and partial autocorrelation function (PACF) plots to visualize temporal autocorrelation and confirm that a seasonal cycle was present in each series (Figure S1). Although sea level is known to fluctuate in response to El Niño Southern Oscillation (ENSO) forcing, with sea levels generally higher during periods of positive Oceanic Niño Index (ONI) and lower during periods of negative ONI, the autocorrelation structure of the time series did not suggest regular multi-annual ENSO driven cycles were present.

To visualize seasonal sea-level variability, we plotted the mean of MMSL residuals from the long-term trend for each month of the year at each station (e.g., see Figure 6). We then calculated the average seasonal range for each station by subtracting the minimum average MMSL deviation value from the maximum average MMSL deviation value. We also calculated the annual total of the magnitude of average monthly change (C) for each station using the equation: $C = \sum_{i=1}^{11} |D_i - D_{i+1}|$, where D is the average MMSL residual values for month i (Table 2). To characterize long-term trends, we used ordinary least squares regression to model linear trends in MMSL across the monitoring period (Figure 4; Table 3; Figures S2 and S3). To visualize interannual variability, we plotted MMSL values with the average seasonal cycle and linear sea-level trend removed (Figure 7).

2.2 | Long-Term Biological Monitoring Dataset and Site Selection

The MARINe Coastal Biodiversity Survey has been conducted at 190 sites, with each site surveyed consistently every 3–5 years since 2001. Survey protocols are described in detail on the MARINe website (Multi-Agency Rocky Intertidal Network (MARINe) Survey Methods n.d.). Briefly, the CBS typically consists of 11 cross-shore transects placed uniformly to form a single large plot at each site (~30 m along-shore × 20–100 m across-shore), along each of which 100 pts. are sampled uniformly. Plots are also topographically mapped so all biological data are linked to tidal elevation. Elevations along every transect were measured using a Trimble GPS system referencing NAVD88 and were converted to MLLW using NOAA's VDatum Tool (NOAA's Vertical Datum Transformation Tool (VDatum v. 4.7) n.d.). Surveys either are "first point contact," in which species identifications of the top layer are collected, or "full point contact," in which up to two additional layers are identified below the top layer. Coastal Biodiversity Surveys are conducted by field teams with advanced taxonomic expertise, and identifications are typically made for all benthic species to
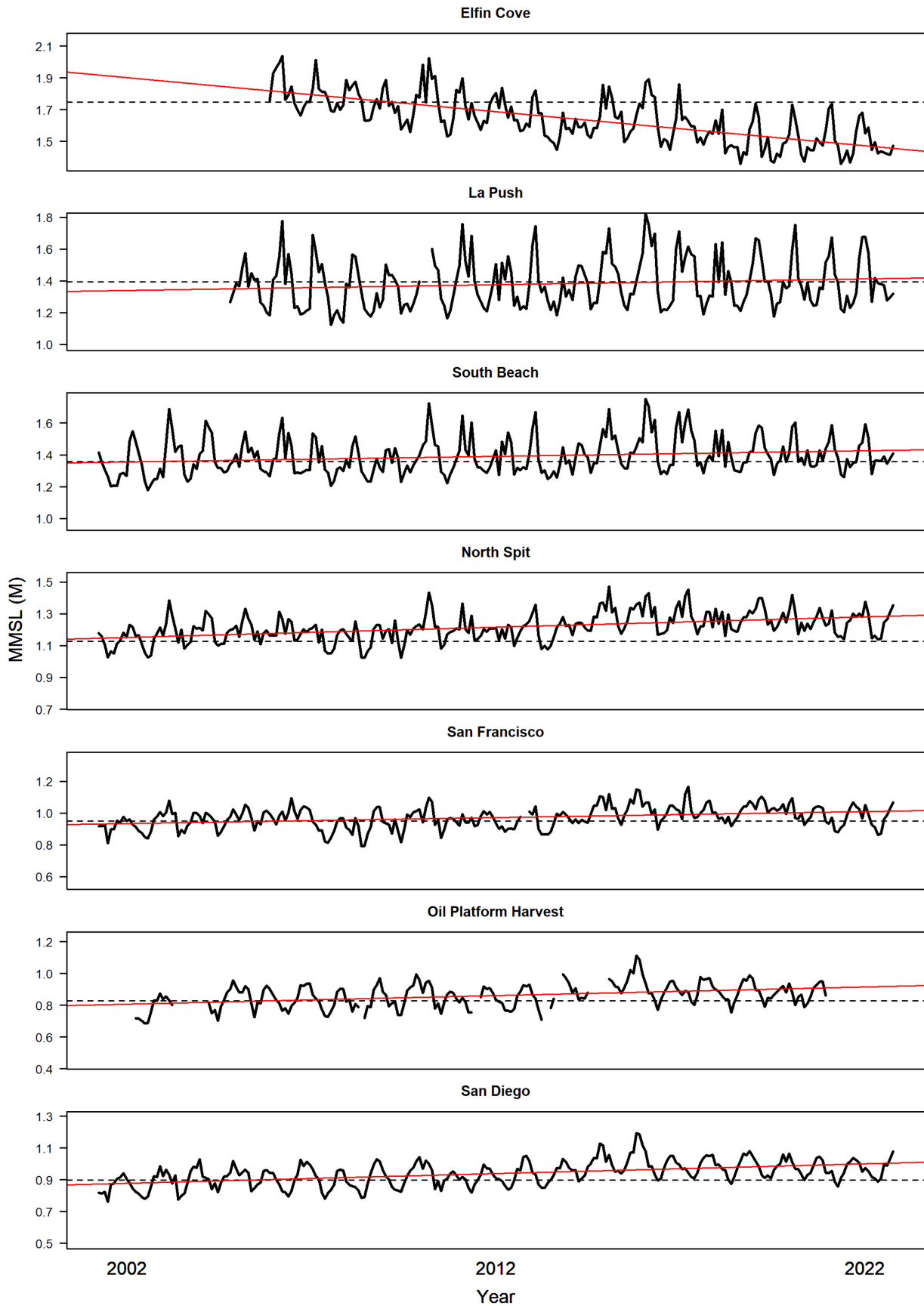
FIGURE 4 | Time series plots of monthly mean sea-level values at seven tide gauge stations (one per region) during the Coastal Biodiversity Survey Monitoring Period (2001–2022). Data values are in reference to mean lower low water (MLLW) at each station, and mean sea level (MSL) is shown (dotted line). Stations with the largest significant sea-level trend for each region are plotted.
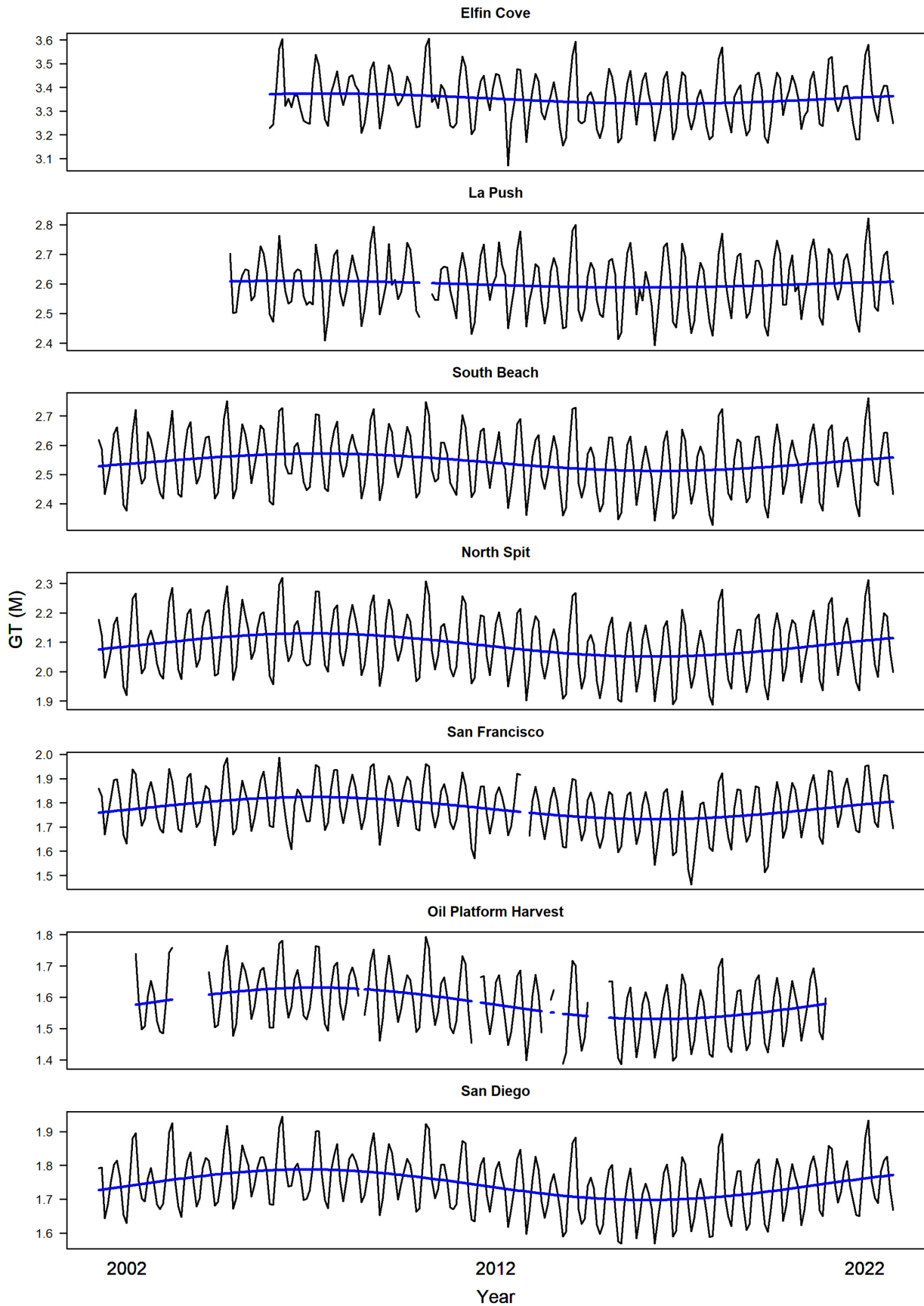
FIGURE 5 | Time series plots of great diurnal range (gt) with fitted sinusoidal function for the Coastal Biodiversity Survey monitoring period (2001–2022). Data values are in reference to mean lower low water (MLLW) at each station, gt is shown with the black line, and the fitted curve representing lunar declination is shown in blue. The same stations from Figure 4 are plotted (one for each region).
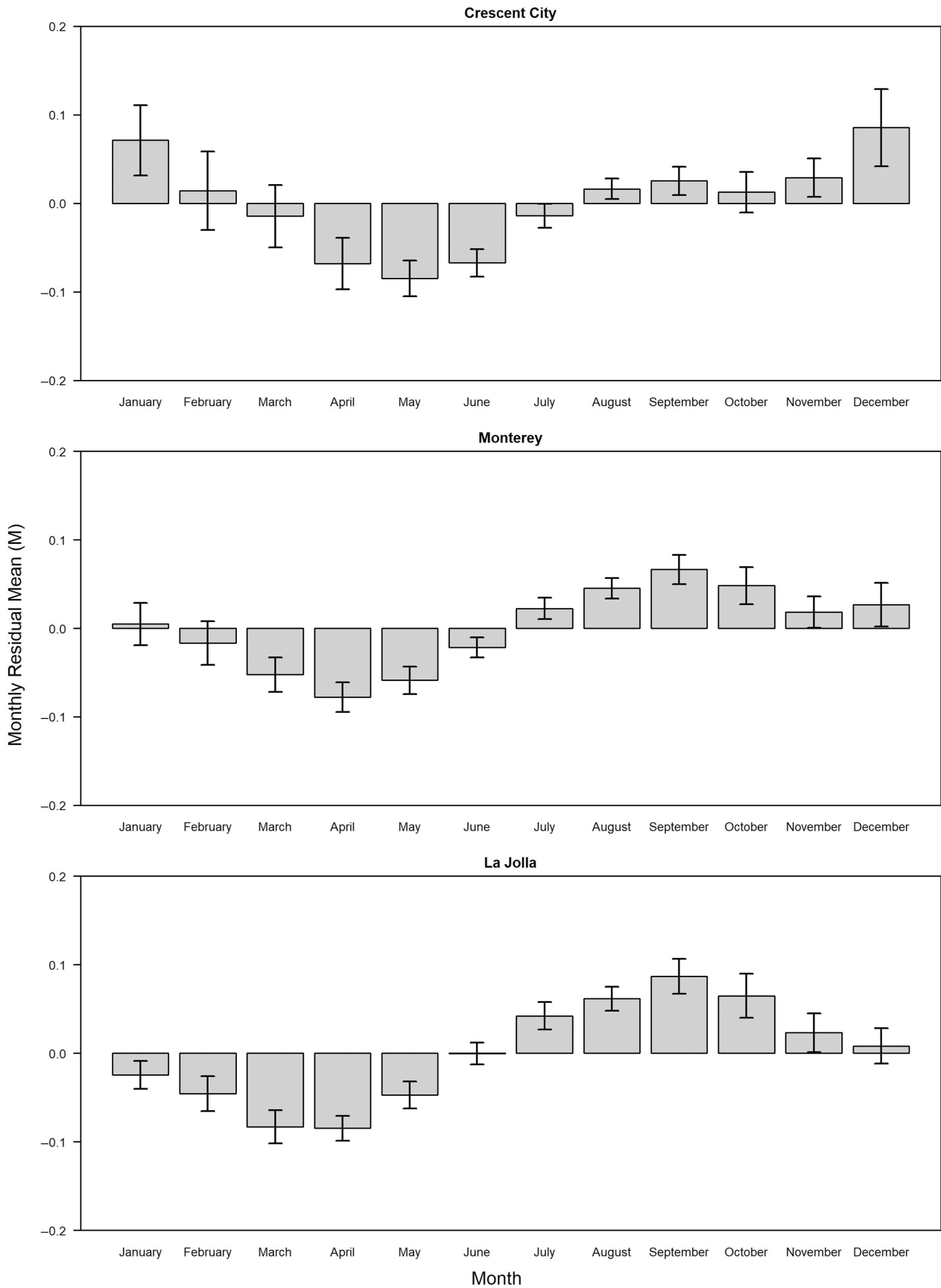
FIGURE 6 | Average seasonal cycle of sea level for 3 of 26 west coast tide gauge stations. Bars indicate mean of the deviation of monthly mean sea-level (MMSL) from the long-term trend estimate for each month of the year ($\pm 1.96 \times SE$).

TABLE 2 | Seasonal trends in MMSL at West Coast tide gauge stations. Arrows indicate whether average of monthly mean sea-level (MMSL) drops or rises between months. Annual peaks are depicted in dark red, and secondary peaks are depicted in light red. Annual troughs are depicted in dark blue, and secondary troughs are depicted in light blue. The seasonal range (maximum average MMSL–minimum average MMSL) is provided to show the magnitude of seasonal variability.

| Region	Tide gauge station	Dec–Jan	Jan–Feb	Feb–Mar	Mar–Apr	Apr–May	May–Jun	Jun–Jul	Jul–Aug	Aug–Sept	Sept–Oct	Oct–Nov	Nov–Dec	Seasonal range (cm)	Total annual change (cm)
Southeast Alaska	Elfin Cove	←	→	→	→	→	←	→	←	←	←	←	←	23	46
	Sitka	→	→	→	→	→	←	→	←	←	←	←	←	24	47
	Port Alexander	←	→	→	→	→	←	←	←	←	←	←	→	22	47
	Ketchikan	→	←	←	→	→	←	→	←	←	←	←	→	23	47
British Columbia															
Washington	Neah Bay	←	→	←	→	→	→	→	←	←	←	←	←	24	51
	La Push	←	→	←	→	→	→	→	←	←	←	←	←	35	74
	Westport	←	→	←	→	→	→	→	←	←	←	←	←	25	51
	Toke Point	→	→	←	→	→	→	→	←	←	←	←	←	32	66
Oregon	Astoria	←	→	←	→	→	→	←	←	←	←	←	←	23	47
	Garibaldi	←	→	←	→	→	→	←	←	←	←	←	←	25	51
	South Beach	→	→	→	→	→	→	←	←	←	←	←	←	23	47
	Charleston	→	→	→	→	→	→	←	←	←	←	←	←	21	41
	Port Orford	→	→	→	→	→	→	←	←	←	←	←	←	19	39
North California	Crescent City	→	→	→	→	→	←	←	←	←	→	←	←	17	36
	North Spit	→	→	→	→	→	←	←	←	←	→	←	←	16	34
North Central California	Arena Cove	→	→	→	→	←	←	←	←	←	→	→	←	17	37
	Point Reyes	→	→	→	→	←	←	←	←	←	→	→	←	15	35
	San Francisco	→	→	→	→	←	←	←	←	←	→	→	←	13	30
South Central California	Monterey	→	→	→	→	←	←	←	←	←	→	→	←	14	30
	Port San Luis	→	→	→	→	←	←	←	←	←	→	→	→	16	33
	Oil Platform Harvest	→	→	→	→	←	←	←	←	←	→	→	→	17	35

(Continues)

RIGHTSLINK

TABLE 2 | (Continued)

Region	Tide gauge station	Dec–Jan	Jan–Feb	Feb–Mar	Mar–Apr	Apr–May	May–Jun	Jun–Jul	Jul–Aug	Aug–Sept	Sept–Oct	Oct–Nov	Nov–Dec	Seasonal range (cm)	Total annual change (cm)
South California	Santa Barbara	→	→	→	←	←	←	←	←	←	→	→	→	16	32
	Santa Monica	→	→	→	→	←	←	←	←	←	→	→	→	16	32
	Los Angeles	→	→	→	→	←	←	←	←	←	→	→	→	16	32
	La Jolla	→	→	→	→	←	←	←	←	←	→	→	→	17	34
	San Diego	→	→	→	←	←	←	←	←	←	→	→	→	17	33

the species level, though coarser taxonomic identifications are sometimes used.

To explore the ecological consequences of sea-level variability, we utilized data from 77 CBS sites (of 190 potential sites) within eight defined regions distributed across 25.5° of latitude (Figure 3). We selected sites that had a minimum of 10 years between initial and final sampling dates. This criterion ensured data were appropriately spread across the temporal extent of interest while also maximizing the number of survey sites. We extracted data for the 10 most abundant benthic taxa (hereafter termed dominant taxa) based on mean percent cover data from each CBS site. Mean % cover was calculated using full point contact data; first point contact data were used only when full point contact samples were not conducted. Of the 245 taxa encountered in the CBS dataset from the 77 sites, 65 were included in the dominant taxa across sites. Identifications included lumped (i.e., functional group) and species level identifications, and three non-biological identifications (rock, sand, tar). This dataset consisted of over half a million (521,510) observations.

This dataset was further filtered based on other data quality criteria before analysis. All surveys in which a taxon was observed fewer than 10 times were dropped to ensure upper limit calculations accurately represented a true limit. All surveys in which tide gauge data from the nearest tide gauge station for the survey month were missing were also dropped. Taxa with limited spatial distributions (only represented by a single tide gauge station or with a latitudinal range < 3°) were dropped. Lumped identifications (i.e., multiple genera within an identification) were also dropped. *Fucus* spp. was retained, as this group contained only species within the same genus that do not have clear geographic delineation and are often indistinguishable in the field. The final dataset contained 22 taxa (plus bare rock and sand) and 977 unique site × survey × taxa combinations. From this dataset, we analyzed 11 taxa targeted by MARINe for monitoring (listed here in order of decreasing available modeling data: *Mytilus californianus*, *Endocladia muricata*, *Balanus glandula*, *Phyllospadix torreyi* S. Watson, 1879, *Silvetia compressa* (J. Agardh) E. Serrão, T.O. Cho, S.M. Boo & Brawley, 1999, *Egregia menziesii* (Turner) Areschoug, 1876, *Fucus* spp., *Tetraclita rubescens* Nilsson-Cantell, 1931, *Phyllospadix scouleri* W.J. Hooker, 1838, *Anthopleura elegantissima* (Brandt, 1835), and *Anthopleura xanthogrammica* (Brandt, 1835)). The full criteria for selecting target species are available on the MARINe website but include the following: species ecologically important in structuring intertidal communities competitive dominants, or major predators; species that are abundant, conspicuous, or large; and species whose presence provides numerous microhabitats for other organisms (Pacific Rocky Intertidal Monitoring: Target Species n.d.). Although *A. xanthogrammica* met our filtering criteria, it was not encountered in enough surveys to produce a model. We also reported results for the upper limit of bare rock as a proxy for the upper limit of biology, as this value is indicative of the elevation of the splash zone above the distribution of most marine species.

2.3 | Changes in Vertical Distribution

Multiple linear regression was used to evaluate whether the upper limits of vertical distribution of the dominant taxa of

TABLE 3 | West Coast tide gauge stations, with regression results. Trend equivalents are provided for the 21.75year monitoring period and for one century and are rounded to the nearest whole cm.

Region	No. of MARINe CBS Sites/Region	No. of MARINe CBS Sites/Tide Gauge	Tide gauge station name	Tide gauge station id	Latitude	Longitude	Model	p	R^2	F-statistic	DF	Trend equivalent (cm/monitoring period)	Trend equivalent (cm/century)
Southeast Alaska	1	0	Elfin Cove	9452634	58.195	−136.347	$y=-0.0018x+1.919$	0***	0.476	183.700	1,202	−47	−216
		1	Sitka	9451600	57.052	−135.343	$y=-0.0005x+1.614$	0***	0.110	32.110	1,259	−13	−60
		0	Port Alexander	9451054	56.247	−134.648	$y=-0.0004x+1.7306$	0.00551**	0.043	7.899	1,176	−10	−48
		0	Ketchikan	9450460	55.332	−131.627	$y=-0.0001x+2.444$	0.248	0.005	1.339	1,259	−3	−12
British Columbia	1	NA											
Washington	2	1	Neah Bay	9443090	48.370	−124.602	$y=-0.000047x+1.275$	0.628	0.001	0.235	1,258	−1	−6
		2	La Push	9442396	47.913	−124.637	$y=0.0003162x+1.3345$	0.0567.	0.017	3.671	1,213	8	38
		0	Westport	9441102	46.905	−124.105	$y=0.0001988x+1.4371$	0.198	0.008	1.668	1,195	5	24
		0	Toke Point	9440910	46.708	−123.967	$y=-0.0000088x+1.4464$	0.939	0.000	0.006	1,252	0	−1
Oregon	4	1	Astoria	9439040	46.207	−123.768	$y=0.00023x+1.343$	0.0138*	0.023	6.143	1,259	6	28
		0	Garibaldi	9437540	45.555	−123.918	$y=0.0002618x+1.343$	0.0646.	0.017	3.452	1,203	7	31
		2	South Beach	9435380	44.625	−124.045	$y=0.000294x+1.352$	0.00166**	0.038	10.110	1,258	8	35
		1	Charleston	9432780	43.345	−124.322	$y=0.0001364x+1.236$	0.099.	0.011	2.741	1,258	4	16
North California	4	0	Port Orford	9431647	42.738	−124.498	$y=-0.0000475x+1.193$	0.614	0.001	0.255	1,241	−1	−6
		2	Crescent City	9419750	41.745	−124.185	$y=-0.0000843x+1.104$	0.58	0.001	0.305	1,258	−1	−5
North Central California	11	2	North Spit	9418767	40.767	−124.217	$y=0.000525x+1.148$	0***	0.203	65.680	1,258	14	63
		4	Arena Cove	9416841	38.915	−123.712	$y=0.0002476x+0.9486$	0.000134***	0.055	15.030	1,258	6	30
		4	Point Reyes	9415020	37.995	−122.973	$y=0.0002854x+0.9393$	0***	0.087	24.540	1,256	7	34
		3	San Francisco	9414290	37.807	−122.465	$y=0.0003075x+0.9318$	0***	0.116	33.710	1,257	8	37
South Central California	26	12	Monterey	9413450	36.605	−121.888	$y=0.0003102x+0.8425$	0***	0.125	36.980	1,258	8	37
		7	Port San Luis	9412110	35.168	−120.753	$y=0.0003021x+0.8289$	0***	0.111	31.810	1,255	8	36
		7	Oil Platform Harvest	9411406	34.470	−120.682	$y=0.0004487x+0.8016$	0***	0.150	35.340	1,201	12	54

(Continues)

RIGHTSLINK()

TABLE 3 | (Continued)

Region	No. of MARINe CBS Sites/ Region	No. of MARINe CBS Sites/ Tide Gauge	Tide gauge station name	Tide gauge station id	Latitude	Longitude	Model	p	R^2	F-statistic	DF	Trend equivalent (cm/ monitoring period)	Trend equivalent (cm/ century)
South California/ Channel Islands	28	8	Santa Barbara	9411340	34.405	−119.693	$y=0.0003787x+0.8264$	0***	0.101	22.810	1,203	10	45
		3	Santa Monica	9410840	34.008	−118.500	$y=0.0002985x+0.8447$	0***	0.105	30.150	1,258	8	36
		14	Los Angeles	9410660	33.720	−118.273	$y=0.0003239x+0.8469$	0***	0.125	36.880	1,259	8	39
		1	La Jolla	9410230	32.867	−117.257	$y=0.0002451x+0.8211$	0***	0.066	18.200	1,257	6	29
		2	San Diego	9410170	32.713	−117.173	$y=0.0004990x+0.8738$	0***	0.237	79.990	1,258	13	60

Note: Statistical significance codes: 0 '***', 0.001 '**', 0.01 '*', 0.05 '.'. Rows in gray have nonsignificant trends. Trend equivalents are as follows: cm of sea-level change in one century, and cm of sea-level change in the monitoring period (2001/01–2022/09, 261 months). Model expressed as sea-level change = m × month + intercept.

interest have shifted in response to sea-level variability during the monitoring period. For response variables, we calculated two metrics from CBS survey point contact data to describe the upper limit of distribution (Z) of each taxon during each CBS survey date at each site. We utilized metrics describing the upper limits of distribution based on the widely supported idea that the upper limits of distribution of intertidal taxa are primarily determined by abiotic factors (i.e., "Connell's Rule," Connell 1961). For taxa that occupy middle to upper intertidal zones and whose vertical distribution is wholly captured by the CBS sampling, we calculated 90th percentile tidal elevation values in reference to MLLW. For taxa that occupy the lower intertidal zone and whose vertical distribution extends below the CBS sampling, we ranked the tidal elevation values in descending order, then calculated the average of the top 10 elevation values in reference to MLLW, as there is no way to calculate an accurate percentile value without observing the lower limit of distribution.

We decomposed the sea-level time series from tide gauge stations nearest the CBS sites into multiple components to serve as potential predictor variables. Sea-level anomalies on the NPC are spatially coherent over large scales (100's of km) so linking CBS data to tide gauge data from the nearest stations is justified (Enfield and Allen 1979). The predictor variables were as follows: the fitted value from the long-term linear trend for the survey month (S), the residual from the long-term linear trend for the survey month (d), the mean of the residuals from the long-term linear trend for the 12 months preceding the survey month (đ), the maximum MMSL value from the 12 months preceding the survey month (M), and the minimum MMSL value from the 12 months preceding the survey month (L). To account for the effect of lunar declination, we fit a sinusoidal function with a period of 18.61 years to the monthly great diurnal range (gt) values for each tide gauge station using ordinary least squares regression (Figure 5). Great diurnal range is a standard NOAA COOPS datum that is the difference between the arithmetic mean of all higher high water (MHHW) values and the arithmetic mean of all lower low water values (MLLW) values observed in any period. The fitted values from this function (termed lunar declination, ld) were extracted for each survey month as an additional predictor variable. To account for variation associated with geography, longitude (x) and latitude (y) were also used as predictor variables. Although other climatic variables, such as sea-surface temperature, wave height, air temperature, and precipitation, also exhibit cyclicity and long-term trends, the focus of this study was on differentiating between the effects of long-term sea-level rise and cyclical variation in sea level at multiple temporal scales. Obtaining local, small-scale climate data matched to each of our survey sites was not possible. As a result, we were not able to include these other climatic variables as potential predictor variables. To some extent, spatial variation in these environmental predictors is accounted for by including longitude and latitude in our model. Multiple regression models were initially built for Z varying as a function of all eight of these predictor variables.

Using variance-inflation factors (VIFs), we found substantial collinearity among predictor variables. Therefore, principal component analysis with varimax rotation was used to develop independent predictor variables (PC Factors) from the data used in the model for each taxon. From the original eight predictor
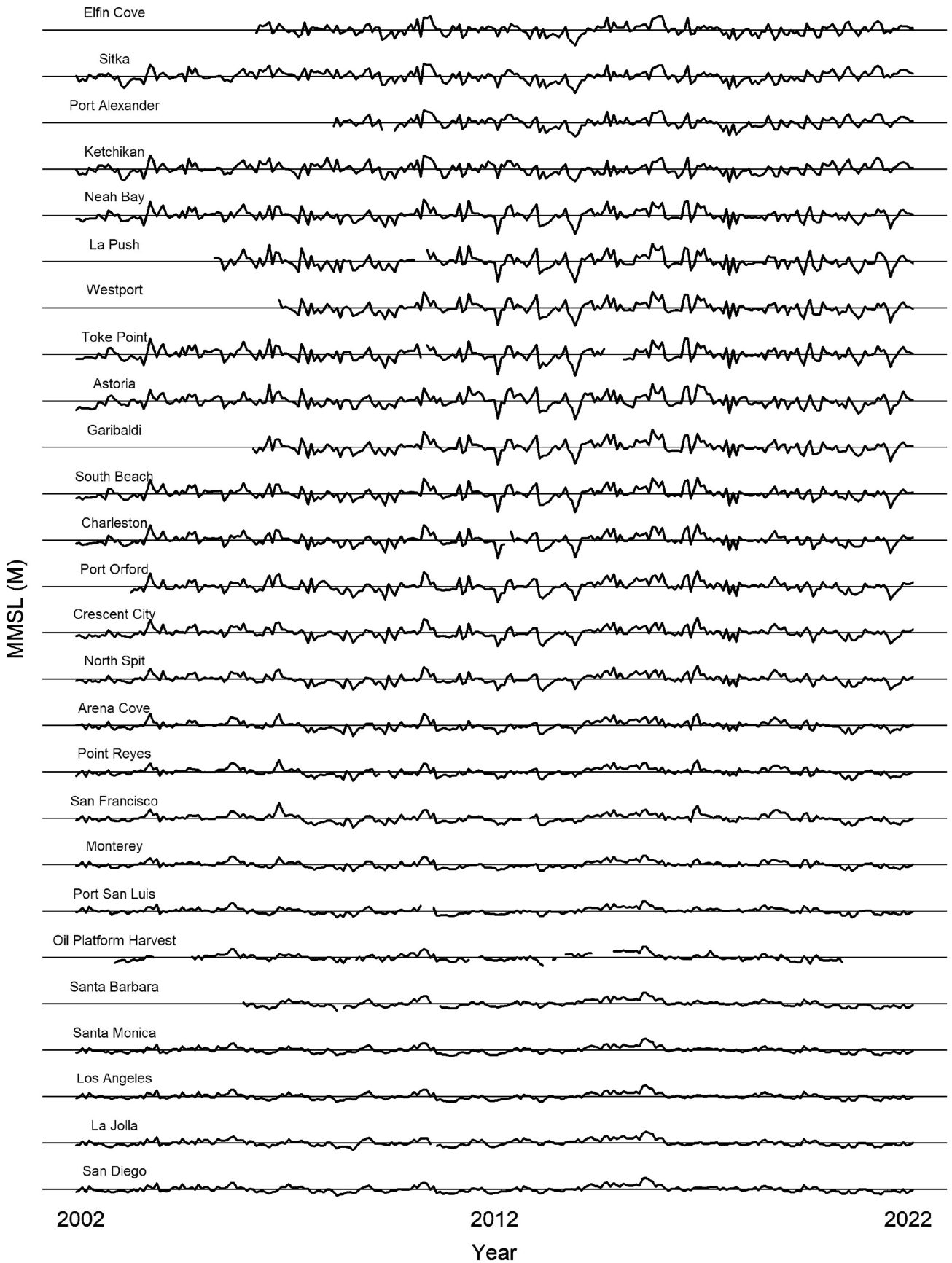
FIGURE 7 | Interannual variability of monthly mean sea level at 26 tide gauge stations. Plots show monthly mean sea-level (MMSL) values with the average seasonal cycle and linear sea-level trend (S) removed, and with the y-axes limited to −0.2 to +0.2 M in reference to mean sea level (MSL). Interannual variability is known to be caused by irregular fluctuations in coastal oceanographic conditions such as ocean temperatures, salinity, and currents. Interannual variability is also tied to the El Niño Southern Oscillation (ENSO).

variables, two principal component axes (PC1 and PC2) were explanatory (eigenvalue ≫ 1) in all cases, except for *T. rubescens*, where three principal component axes were explanatory. Loadings varied by taxa (Table 4). For eight of the eleven models run, S, M, L, and ld loaded strongly positively on PC1, and a combination of these variables, but not all of them, loaded strongly positively on PC1 for the other three models. As a result, PC1 represents the effect of lunar declination and the long-term sea-level trend with negative values being small average tidal amplitudes and lower sea levels and positive values being large average tidal amplitudes and higher sea levels. Latitude loaded strongly positively, and longitude loaded strongly negatively on PC2 for three models. Thus, PC2 represents the CBS site geographic location, with negative values being south-easterly and positive values being north-westerly. The residual

values (d and đ) were orphan variables in all models, not loading strongly (value close to 0) on PC axes, except for in the *T. rubescens* model, where đ loaded strongly positively on PC3, along with M. Longitude was an orphan variable in all cases in which it did not load on PC2 (Table 4). We used a stepwise regression approach to model simplification (both directions), selecting the most parsimonious model with the lowest Aikaike-information criterion (AIC) score for each of the taxa (Table 4). The results from these final models are reported (Tables 5 and 6). Partial residual plots were created for the models with multiple significant terms to visualize the effects of each significant term on upper limits individually (Figures 8–12). We conducted all quantitative data summaries, analyses, plotting, and mapping using R (R Core Team 2021). All data and code for these analyses are openly available online (Kaplanis 2024).

TABLE 4 | Principal component loadings for all taxa models. Table shows where explanatory variables load on principal component axes and whether the loading is + or −, the orphan variables for each model, and the terms retained in the final stepwise regression models as well as their AIC scores.

Taxa	Principal component axis	Variable loadings +	Variable loadings −	Orphans	Final model	AIC
Balanus glandula	PC1	y, S, L, M, ld		x, d, đ	$Z \sim PC1 + x + d + đ$	−75.04
Bare Rock	PC1	y, S, L, M, ld		x, d, đ	$Z \sim PC1 + x$	−120.6
Endocladia muricata	PC1	y, S, L, M, ld		x, d, đ	$Z \sim PC1 + x + d + đ$	−137.9
Fucus spp.	PC1	y, S, L, M, ld		x, d, đ	$Z \sim PC1 + x + d$	−59.66
Mytilus californianus	PC1	y, S, L, M, ld		x, d, đ	$Z \sim PC1 + x + d + đ$	−205.4
Anthopleura elegantissima	PC1	y, S, L, M, ld		x, d, đ	$Z \sim PC1 + x$	−21.88
Tetraclita rubescens	PC1	S, L		d, ld	$Z \sim PC2$	−51.81
	PC2	y	x			
	PC3	M, đ				
Silvetia compressa	PC1	S, L, M		d, đ, ld	$Z \sim PC1 + PC2 + ld$	−70.2
	PC2	y	x			
Phyllospadix scouleri	PC1	y, S, L, M, ld		x, d, đ	$Z \sim x$	−69.19
Egregia menziesii	PC1	S, L, M, ld		d, đ	$Z \sim PC2$	−56.93
	PC2	y	x			
Phyllospadix torreyi	PC1	y, S, L, M, ld		x, d, đ	$Z \sim PC1 + x$	−89.51

Variable	Symbol	Class
Latitude	y	Explanatory
Longitude	x	
Long-term linear trend	S	
Preceding year minimum MMSL	L	
Preceding year maximum MMSL	M	
Survey month residual	d	
Preceding year residual mean	đ	
Lunar declination	ld	
Species upper limit	Z	Response

TABLE 5 | Intertidal taxa responses to sea-level variability. Results presented from multiple linear regression models evaluating response of upper limits (Z, ninetieth percentile and mean of 10 highest observations) of 10 taxa and bare rock to multiple model terms.

Taxa	Response variable	Mean upper limit (m+MLLW ± SE)	Model component	Sign	Estimate	Std. error	t-Value	p	Sign. code	R²	DF	F-statistic	Model p-value
Balanus glandula	Ninetieth percentile	2.119±0.106	Intercept	+	−10.60367	2.73851	−3.872	3.08E-04	***	0.615	4,51	23	7.01E-11
			Lunar declination + trend	+	0.17261	0.08005	2.156	3.58E-02	*				
			Longitude	−	−0.10231	0.02244	−4.559	3.25E-05	***				
			Residual	−	−2.91244	1.23039	−2.367	0.021761	*				
			Preceding year residual mean	+	8.60712	2.64674	3.252	0.002035	**				
Bare Rock	Ninetieth percentile	1.851±0.06	Intercept	−	−11.7736	2.65567	−4.433	1.57E-05	***	0.239	2,189	31	2.35E-12
			Lunar declination + trend	+	0.18331	0.05821	3.149	0.0019	**				
			Longitude	−	−0.11191	0.02181	−5.131	7.10E-07	***				
Endocladia muricata	Ninetieth percentile	1.525±0.059	Intercept	+	−11.137	4.929	−2.259	0.026	*	0.325	4,92	13	3.48E-08
			Lunar declination + trend	+	0.184	0.056	3.299	0.001	**				
			Longitude	−	−0.103	0.040	−2.554	0.012	*				
			Residual	−	−1.804	0.967	−1.867	0.065					
			Preceding year residual mean	−	−2.892	1.948	−1.485	0.141					
Fucus spp.	Ninetieth percentile	1.428±0.154	Intercept	−	−12.23038	3.1423	−3.892	0.000536	***	0.814	3,29	48	2.48E-11
			Lunar declination + trend	+	0.44969	0.0791	5.685	3.79E-06	***				
			Longitude	−	−0.10802	0.02547	−4.241	0.000207	***				
			Residual	−	−3.94278	1.39147	−2.834	0.008293	**				
Mytilus californianus	Ninetieth percentile	1.383±0.052	Intercept	−	−14.842	2.558	−5.802	0.000	***	0.405	4,133	24	4.16E-15
			Lunar declination + trend	+	0.117	0.044	2.642	0.009	**				
			Longitude	−	−0.133	0.021	−6.304	0.000	***				
			Residual	−	−1.568	0.804	−1.950	0.053					
			Preceding year residual mean	+	2.153	1.521	1.416	0.159					
Anthopleura elegantissima	Ninetieth percentile	1.188±0.129	Intercept	−	−19.28072	11.54367	−1.67	0.1084		0.105	2,23	2.5	0.1076
			Lunar declination + trend	−	−0.26634	0.13673	−1.948	0.0637					
			Longitude	−	−0.16786	0.09466	−1.773	8.94E-02					
Tetraclita rubescens	Ninetieth percentile	0.933±0.09	Intercept	+	0.93339	0.0683	13.667	1.58E-12	***	0.407	1,23	17	0.000359
			Geography	+	0.29144	0.06971	4.181	0.000359	***				

(Continues)

TABLE 5 | (Continued)

Taxa	Response variable	Mean upper limit (m + MLLW ± SE)	Model component	Sign	Estimate	Std. error	t-Value	p	Sign. code	R²	DF	F-statistic	Model p-value
Silvetia compressa	Ninetieth percentile	0.847±0.109	Intercept	+	7.0734	2.06777	3.421	0.00138	**	0.632	3,43	27	4.69E-10
			Trend	−	-0.19385	0.06981	-2.777	0.0081	**				
			Geography	+	0.51597	0.06709	7.691	1.31E-09	***				
			Lunar declination	−	-3.76778	1.25069	-3.013	0.00433	**				
Phyllospadix scouleri	Mean top 10	0.73±0.08	Intercept	−	-18.6149	4.4543	-4.179	0.000137	***	0.284	1,44	19	8.13E-05
			Longitude	−	-0.1572	0.0362	-4.344	8.13E-05	***				
Egregia menziesii	Mean top 10	0.237±0.095	Intercept	+	0.2372	0.0769	3.085	0.00364	**	0.352	1,41	24	1.64E-05
			Geography	+	0.37977	0.07781	4.881	1.64E-05	***				
Phyllospadix torreyi	Mean top 10	0.093±0.077	Intercept	−	-22.00287	3.34357	-6.581	4.28E-08	***	0.484	2,45	23	1.31E-07
			Lunar declination + trend	−	-0.2106	0.05886	-3.578	0.000843	***				
			Longitude	−	-0.18355	0.02777	-6.609	3.88E-08	***				

Note: Statistical significance codes: ***<0.001, **<0.01, *<0.05, .<0.1.

3 | Results

3.1 | Sea-Level Variability—Seasonality

All stations exhibit seasonal sea-level variability, and the timing of seasonal peaks and troughs varies geographically (Table 2). From Arena Cove south, sea level is lowest in the spring upwelling season (March–April) and highest during the late summer (September, except for Arena Cove, that peaks in December). Moving from northern California to Washington, the timing of the seasonal low shifts progressively later, from May in North Spit to Port Orford to July in Garibaldi to Neah Bay. In Southeast Alaska, the seasonal low occurs in May, except for in Elfin Cove, where sea level is lowest in July. The seasonal high occurs in December between Arena Cove and South Beach and then shifts to January from Garibaldi to Elfin Cove, with the exception of Toke Point, Ketchikan, and Sitka, where the high occurs in December, November, and December, respectively (Table 2). The magnitude of seasonal sea-level variability also varies geographically. The greatest seasonal variability occurs at La Push (35 cm (range), 74 cm (total change), Table 2), while the least occurs at San Francisco (13 cm (range), 30 cm (total change), Table 2). Regionally, seasonal sea-level variability is largest in Washington and smallest in South Central California (Table 2).

3.2 | Sea-Level Variability—Long-Term Trends

Twenty of twenty-six tide gauge stations had significant sea-level trends (Table 3). All tide gauge stations in California and Oregon had significant SLR except Crescent City and Port Orford. Over the course of the monitoring period, the greatest significant SLR occurred at North Spit, in North California (trend equivalent: 14 cm/monitoring period of 21.75 years or 261 months, from 01/2001 to 09/2022), followed by San Diego, South California (13 cm), then Oil Platform Harvest, South Central California (12 cm). The least SLR (4 cm) occurred at Charleston, Oregon. Only one station in Washington (La Push) had significant SLR (8 cm). Three of four tide gauge stations in Southeast Alaska exhibited significant drops in relative sea level because of continental uplift, from 10 cm at Port Alexander to 47 cm at Elfin Cove.

3.3 | Changes in Vertical Distribution—Sea-Level Trend and Lunar Declination (PC1)

The upper limits of vertical distribution were significantly positively correlated with lunar declination and long-term sea level (PC1) for four taxa (*B. glandula*, *E. muricata*, *Fucus* spp., and *M. californianus*) and bare rock (Figure 8; Table 5). Upper limits were significantly negatively correlated with PC1 for two taxa (*A. elegantissima* and *P. torreyi*; Figure 8; Table 5) and significantly negatively correlated with lunar declination (ld) and sea-level trend (S) separately for *S. compressa* (Figure 9; Table 5).

3.4 | Changes in Vertical Distribution—Geography (PC2) and Longitude (x)

The upper limits of vertical distribution were significantly positively correlated with geography (PC2) for three taxa (*T.
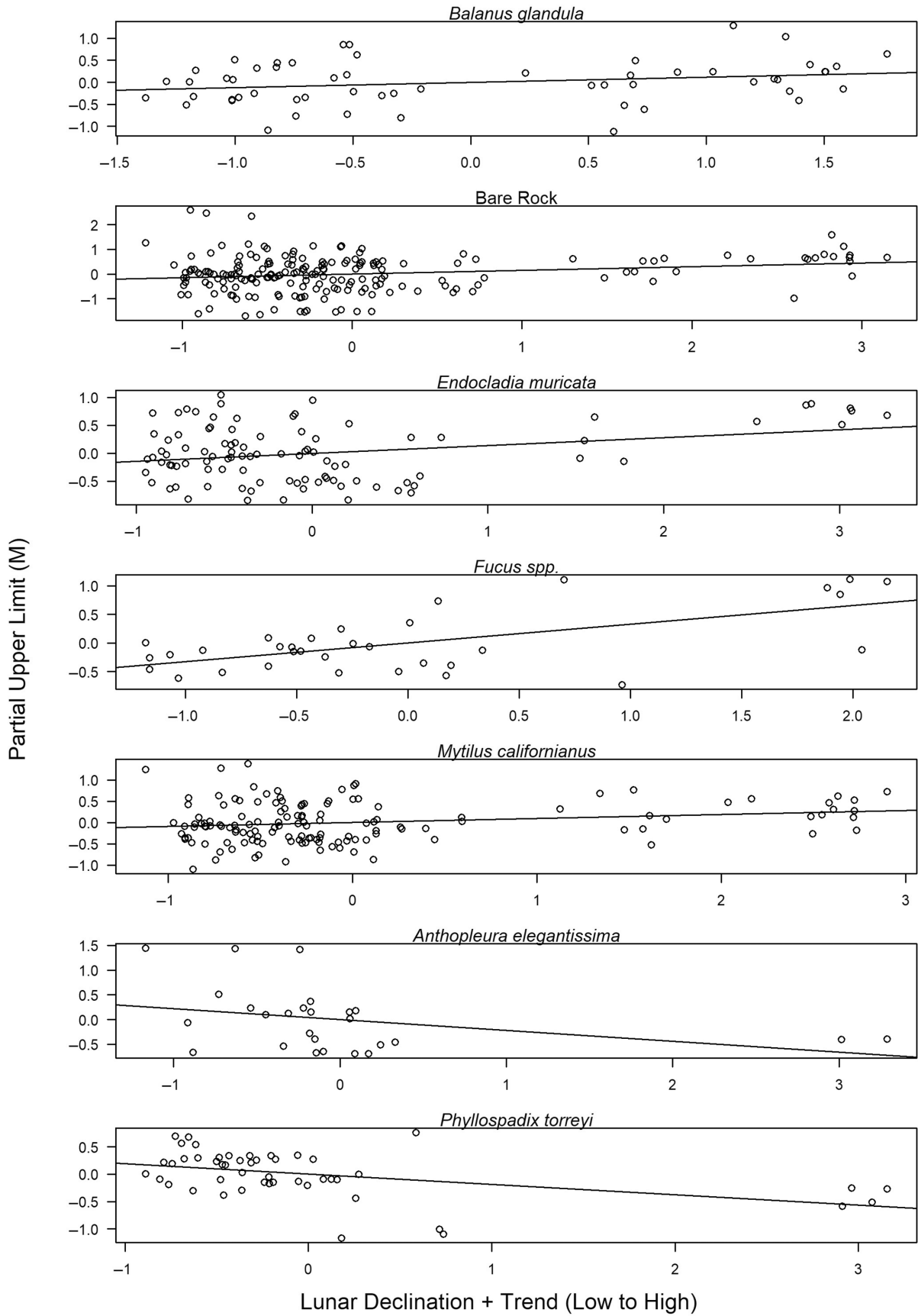
FIGURE 8 | Upper intertidal taxa exhibit positive relationships with lunar declination and sea level, while lower taxa exhibit negative relationships. Plots depict the effect of lunar declination + trend (PC1) on the partial upper limit (90th percentile elevation in meters, except for *P. torreyi*, where upper limit is the mean of the top 10) of six taxa and bare rock, ordered from highest to lowest average upper limit.

TABLE 6 | Summary data for taxa analyzed. Table depicts summary information for data associated with each taxon and bare rock, and statistical significance of terms in multiple linear regression models. Positive relationships are color coded with red while negative relationships are blue.

Taxa	N	No. sites	No. tide gauge stations	Latitudinal range (degrees)	Lunar declination + trend	Lunar declination alone	Trend alone	Geography (latitude + longitude)	Longitude	Residual	Preceding year residual mean
Balanus glandula	56	23	14	23.6	*				***	*	**
Bare Rock	192	74	19	24.5	**				***		x
Endocladia muricata	97	36	13	18.7	**				*		
Fucus spp.	33	9	8	20.9	***				***	**	
Mytilus californianus	138	55	17	19.0	**				***		x
Anthopleura elegantissima	26	10	6	13.6							
Tetraclita rubescens	25	11	3	3.6				***			
Silvetia compressa	47	21	6	6.3		**	**	***			
Phyllospadix scouleri	46	16	11	19.2					***		
Egregia menziesii	43	19	10	7.4				***			
Phyllospadix torreyi	48	22	10	12.2	***				***		
Anthopleura xanthogrammica	5	2	2	10.7							

Note: Statistical significance codes: *** < 0.001, ** < 0.01, * < 0.05, . < 0.1, X = retained, nonsignificant.
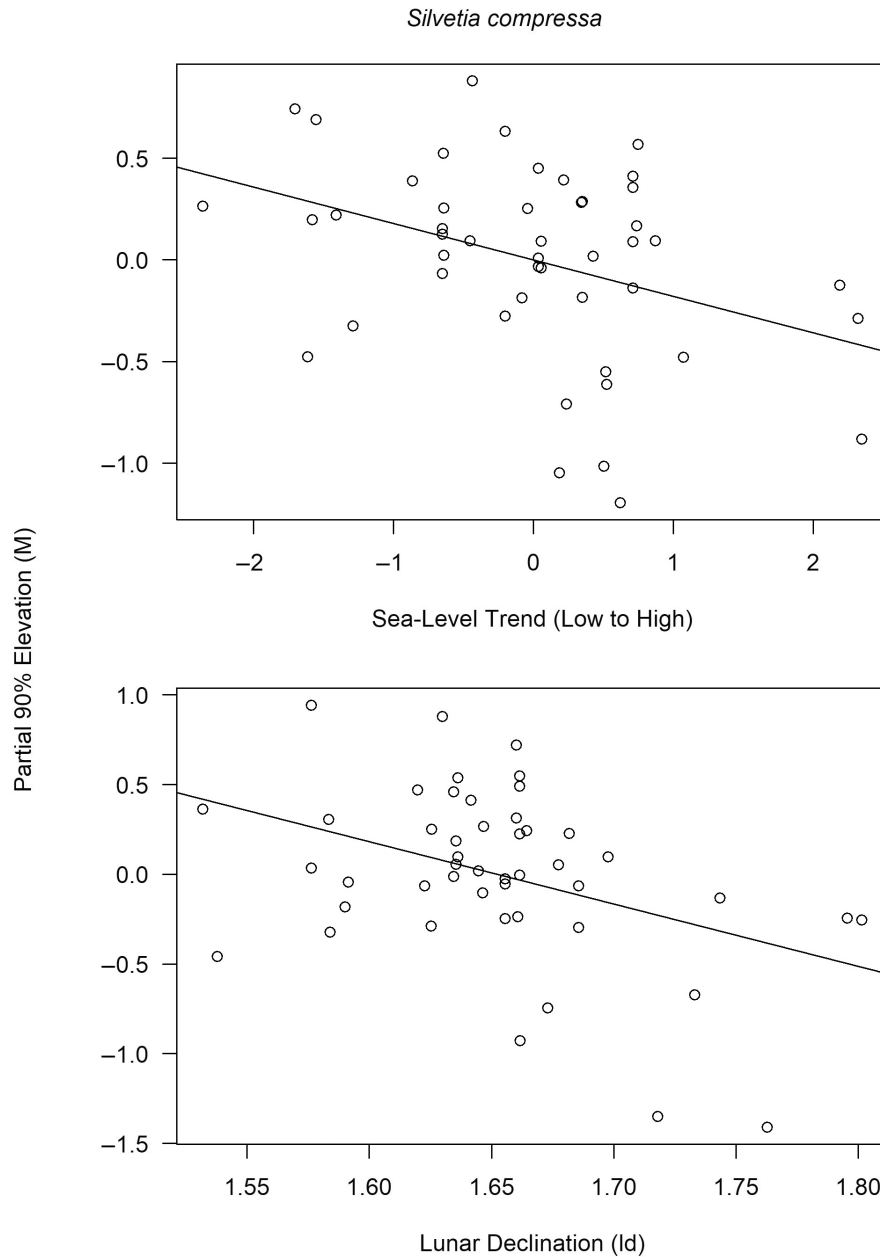
FIGURE 9 | The lower intertidal species *S. compressa* exhibits negative relationships with sea-level trend and lunar declination separately. Plots depict the effect of the long-term sea-level trend (PC1), and lunar declination (ld) on the partial upper limit (90th percentile elevation in meters) of *S. compressa*.

rubescens, *S. compressa*, and *E. menziesii*; Figure 10; Table 5). Upper limits were significantly positively correlated with longitude (x) alone for seven taxa (*B. glandula*, *E. muricata*, *Fucus* spp., *M. californianus*, *A. elegantissima*, *P. scouleri*, and *P. torreyi*) as well as with bare rock (Figure 11; Table 5). Note, that although the sign of the relationship is negative, the correlation is positive from E to W, as longitude is presented with negative values.

3.5 | Changes in Vertical Distribution—Residuals (d) and Preceding Year Residual Mean (đ)

The upper limits of vertical distribution were significantly negatively correlated with residuals (d) for four taxa (*B. glandula*,

E. muricata, *Fucus* spp., and *M. californianus*; Figure 12; Table 5). Taxa showed a mixed response to the preceding year residual mean (đ), with *B. glandula* and *M. californianus* exhibiting a significant positive relationship, and *E. muricata* exhibiting a significant negative relationship (Figure 12; Table 5).

4 | Discussion

4.1 | General Conclusions

The ecological impacts of large-scale, long-term sea-level variability have not been thoroughly examined (Burnaford, Nielsen, and Williams 2014; Denny et al. 2004; Denny and
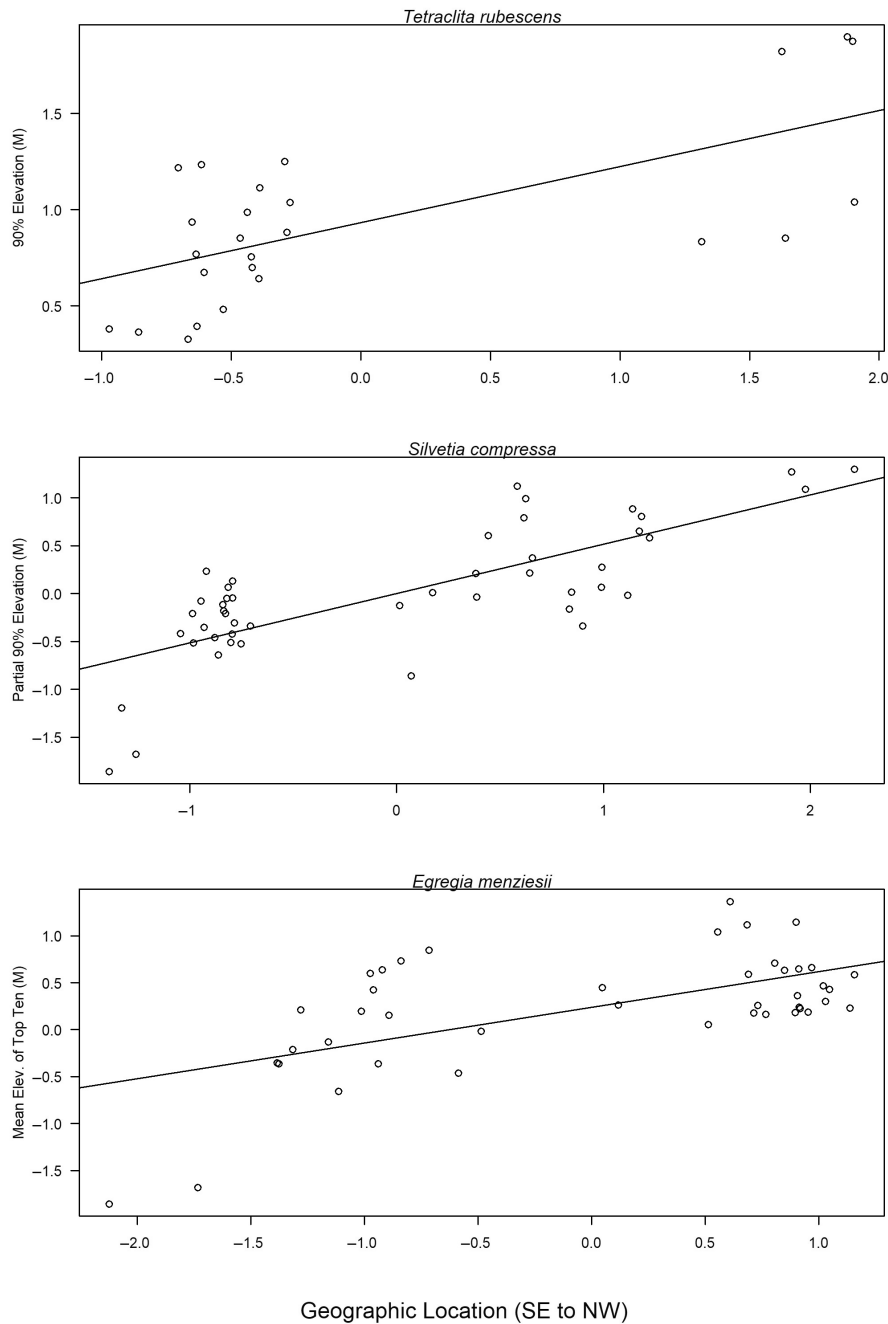
FIGURE 10 | The upper limits of intertidal taxa are higher moving upcoast. Plots depict the effect of geographic location (PC2) on the upper limits (90th percentile elevation in meters, partial 90th percentile elevation, and mean elevation of the top 10 in meters) of *T. rubescens*, *S. compressa*, and *E. menziesii*. The plots are ordered from highest to lowest average upper limit.

Paine 1998). This paper provides a characterization of the spatiotemporal scales of sea-level variability on rocky shores of the NPC, new perspective on how rocky intertidal ecosystems respond to this environmental variability, and insight into how these communities may respond to SLR in coming years. This work also demonstrates the value of long-term and large-extent environmental and biological monitoring programs for understanding the ecological impacts of long-term climate change and cyclical environmental variability. The rocky intertidal zone of the NPC is one of the most thoroughly monitored ecosystems in the world in terms of spatial

and temporal extent and resolution of ecological data, and of the numerous programs that have collected data in this area, MARINe has the most expansive and resolved dataset (Kaplanis et al. 2020). Detecting vertical distribution shifts was only possible due to the high resolution and broad spatial and temporal extent of this dataset. Without these long-term, large-scale data, differentiating the effects of anthropogenic, long-term climate change, and natural cyclical dynamics would be impossible (Harley et al. 2006; Hughes et al. 2017; Kaplanis 2023; Lindenmayer et al. 2012, 2015; Mieszkowska et al. 2014, 2021).
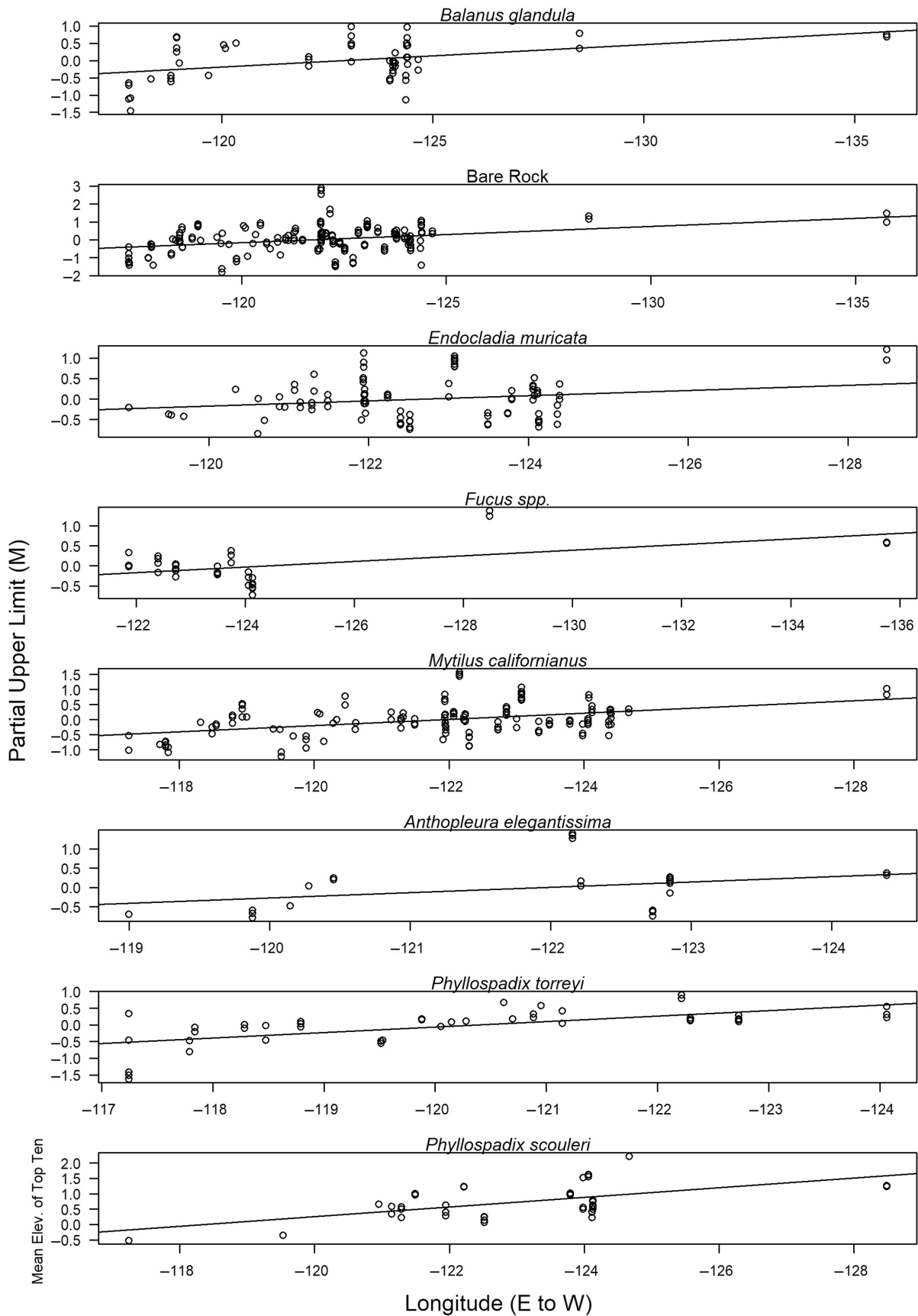
FIGURE 11 | The upper limits of intertidal taxa are higher moving west. Plots depict the effect of longitude (x) on the partial upper limits of seven taxa (90th percentile elevation in meters, except for *P. scouleri* and *P. torreyi*, where upper limit is the mean of the top 10), as well as bare rock. The plots are ordered from highest to lowest average upper limit.
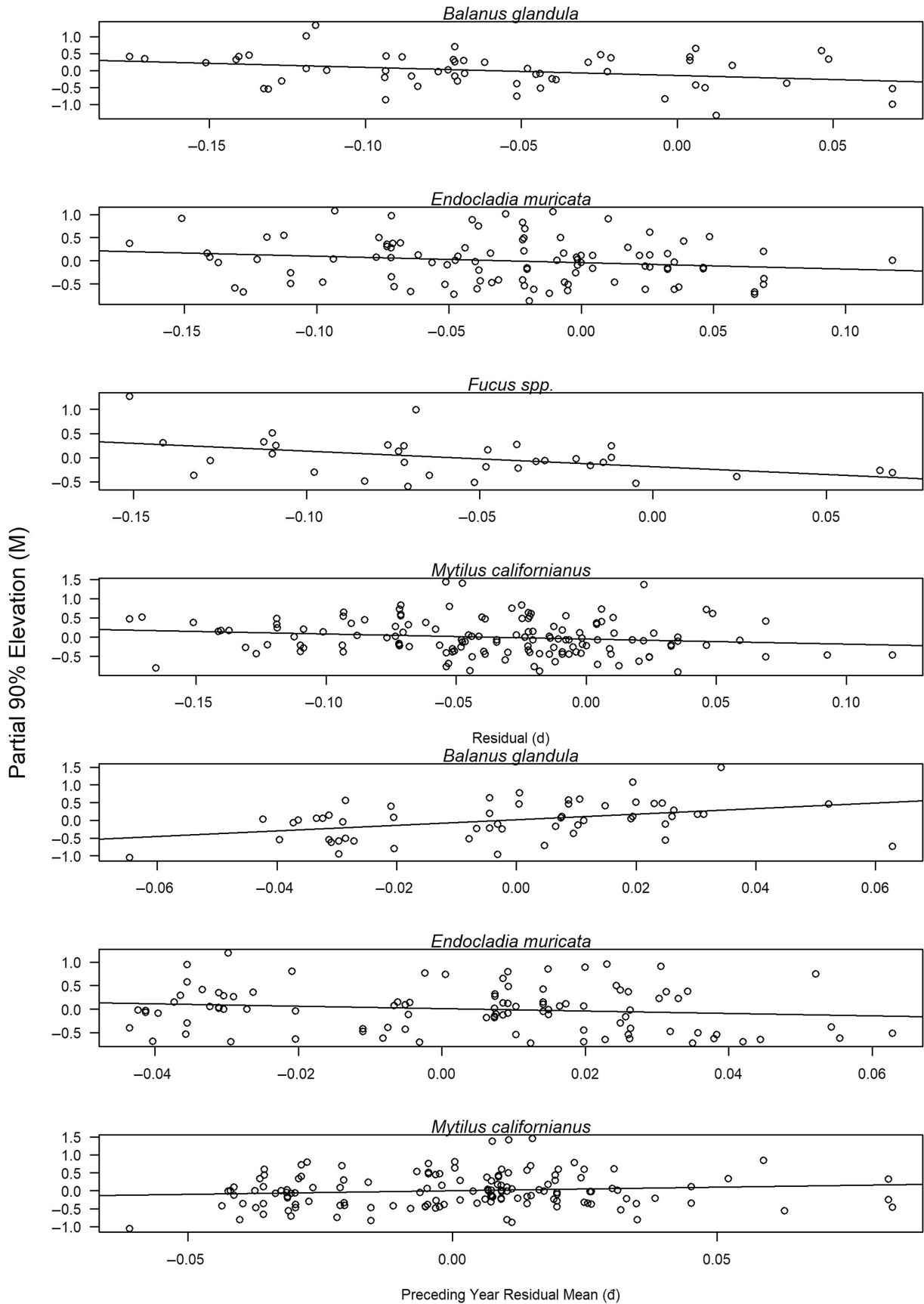
FIGURE 12 | The upper limits of intertidal taxa exhibit negative relationships with residuals, but mixed responses to preceding year residual mean. Plots depict the effect of residual (đ) and preceding year residual mean (đ) on the partial upper limits (90th percentile elevation in meters) of *B. glandula*, *E. muricata*, *Fucus* spp., and *M. californianus*. Plots are ordered by predictor variable, then from highest to lowest average upper limit.

4.2 | Sea-Level Variability—Seasonality

This paper describes sea-level variability observed at tide gauge stations across the west coast, from seasonal to multi-decadal scales. We found that seasonal variability (13–74 cm) occurs at all stations (Table 2). This seasonal variability is larger in magnitude than the total change exhibited in the long-term trend over the monitoring period for most locations. Yet in our analysis we saw little evidence of a significant correlation between short-term sea-level variability (as represented by residual, d) and upper limits of distribution. Other spatially and temporally variable factors may buffer against the expected effects of short-term sea-level variability on upper limits. From Southeast Alaska to Oregon, sea levels are highest in the winter, but upper limits may not increase due to the counteracting effect of seasonal freezing and nighttime timing of the lowest tides, when the risk of freezing is highest (Stickle et al. 2016). In southern Oregon and California, MMSL values are lowest during the spring upwelling season, and although this drop would be expected to drive down upper limits, the early morning timing of the lowest tides, drops in sea-surface temperature, and wetting by wind-carried spray common during this season may counteract the seasonal sea-level effects (Mislan, Wethey, and Helmuth 2009; Stickle et al. 2016). In North Central to Southern California, sea level is highest in late summer, which would be expected to raise upper limits, but this may be partly counteracted by the coincidental timing of factors that increase the physiological stress associated with low tide emersion including: the smallest waves and swell conditions of the year, peaks in seasonal air temperatures, and the seasonal occurrence of dry, strong, Diablo and Santa Ana winds (Helmuth et al. 2006; Mislan, Wethey, and Helmuth 2009). Ultimately, organisms may not rapidly respond to short-term seasonal sea-level variability due to their physiological tolerances to stress and sessile life histories.

4.3 | Sea-Level Variability—Long-Term Trends

Our results are consistent with long-term tide gauge monitoring results and published projections of sea-level rise on the NPC (Cazenave et al. 2014; Chen et al. 2017; Church et al. 2013; Church and White 2006; National Research Council 2012; NOAA Tides and Currents, Relative Sea-Level Trends n.d.; Sweet et al. 2014, 2017), with most tide gauge stations exhibiting substantial sea-level rise during the monitoring period. The magnitude of the SLR during the monitoring period is potentially ecologically relevant. For example, in San Francisco the 8 cm of SLR is 61% of the total seasonal range and 4.5% of the great diurnal range. Interestingly, in southeast Alaska, continental uplift has led to a recorded fall in relative sea level. Further research on whether these trends are causing intertidal species to shift downward would be interesting, but few sites have been consistently monitored within this region due to difficulty of access (Kaplanis 2023).

4.4 | Changes in Vertical Distribution

This paper is the first to quantitatively document that intertidal taxa exhibit shifts in vertical distribution in correlation with multiple components of sea-level variability across the NPC.

Few ecologists have attempted to address this question due to the inherent complexity of sea-level variability and the spatial and temporal extent of data needed to encompass its scales of variability (Burnaford, Nielsen, and Williams 2014; Denny and Paine 1998; Harley and Paine 2009). We found significant relationships between upper limits and multiple components of sea-level variability for a variety of taxa, including sessile invertebrates, brown and red algae, and surfgrasses, that occupy distinct distributions at varying levels across the rocky intertidal zone.

Our most significant finding was that upper intertidal taxa have a significant positive relationship with SLR and lunar declination, while lower intertidal taxa have a significant negative relationship. Unfortunately, disentangling the effects of these two drivers was not possible with our data. Although one would expect a uniform increase in upper limits with SLR, the negative relationship of lower intertidal taxa suggests that, at least for these taxa, variation in tidal amplitude driven by lunar declination may have an overwhelming influence on average sea-level conditions, since their upper limits were observed to be lower when you would expect them to be higher based solely on SLR. We believe the mechanism behind the relationships between lunar declination and upper limits is changes in the relative influence of MHHW and MLHW as they vary with lunar declination. Upper taxa likely move upward with the increase in MHHW associated with increasing lunar declination (early and late in the time series, with maxima in 2006 and 2025). Above a certain height on the shore, only MHHW provides submersion that influences upper limits. Lower taxa likely move upward with the increase in MLHW associated with decreasing lunar declination (minima in 1997 and 2015), which imparts an additional period of submersion or wetting at intermediate to low tidal heights that counteracts the decrease in expected submersion time associated with MHHW dropping.

These results are consistent with those of Denny and Paine (1998), who demonstrated that variation in tidal emersion with changing lunar declination varied substantially with height on the shore. Our results also provide an alternative explanation for the observed upward shifts of *E. muricata* from 1963 to 1970 by Hunt (2006) and of *B. glandula* and *E. muricata* from 1992 to 2002 by Readdie (2004)—that they were driven by shifts from lunar declination minima to maxima in 1959–1968 and 1997–2006. It is worth noting that the taxa exhibiting negative relationships with lunar declination and trend (*A. elegantissima* and *P.* torreyi) have southerly distributions where the effects of lunar declination on tidal amplitude are more pronounced, and thus may more strongly overwhelm any influence of SLR alone (Figures 5 and 13).

The strong influence of cyclical celestial mechanics demonstrated here strengthens the argument previously made against concluding that changes in intertidal community structure or function detected through sampling at disparate timepoints are driven solely by anthropogenic climate change (Burnaford, Nielsen, and Williams 2014; Denny and Paine 1998; Harley and Paine 2009). Cyclical processes at a range of temporal scales can obscure or overwhelm the impacts of long-term climate change. For example, Mislan, Wethey, and Helmuth (2009)
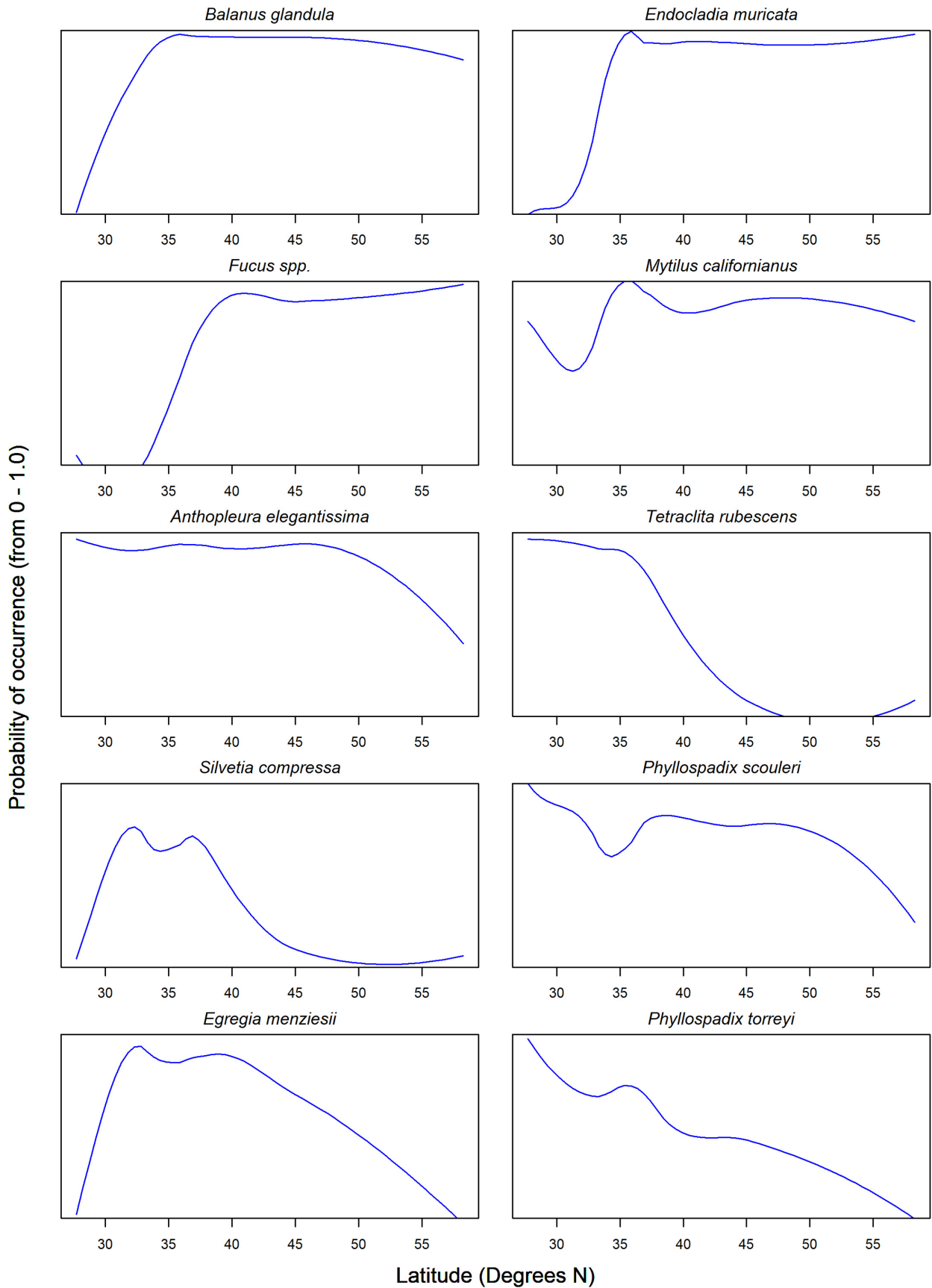
FIGURE 13 | Latitudinal distribution of intertidal taxa. Plots depict the probability of occurrence of taxa as a locally estimated scatterplot smoothing (LOESS) curve fit to presence data collected across all Multi-Agency Rocky Intertidal Network (MARINe) sites.

demonstrated that the frequency of "risky days," in which intertidal organisms experience elevated heat stress due to low tides paired with high air temperatures, exhibits spatial and cyclical temporal variability. In addition, stochastic departures from mean conditions associated with extreme events such as storms and aerial heat waves, alone or in combination, can have significant effects on community composition and vertical distribution entirely independent of SLR and lunar declination (Harley and Paine 2009; Hawkins, Burrows, and Mieszkowska 2023; Hesketh and Harley 2023; Littler and Littler 1987; Mieszkowska et al. 2021; Wethey et al. 2011). For example, Harley and Paine (2009) show that vertical limits of upper intertidal algae exhibit distinct drops when unusually calm seas occur in combination with aerial heat waves, causing dieback in the upper limits. Using long-term data from intertidal sites across the United Kingdom, Mieszkowska et al. (2021) showed that the abundance of invertebrates and macroalgae generally decreased with increasing frequency of winter cold spells and summer heat waves (Mieszkowska et al. 2021). These examples and others suggest that spatially and temporally variable extreme events can complicate or counteract long-term trends. In the future though, the relative influence of SLR may come to dominate over the short-term stochastic events and the lunar declination effect if the rate of SLR accelerates according to forecasts (Chen et al. 2017; Church and White 2006; Sweet et al. 2017). Only continued monitoring of multiple environmental conditions, such as air and water temperatures, in association with biological monitoring will allow us to understand the changing influences of these drivers (Kaplanis 2023). The relationships we found between geography (PC2) and longitude and upper limits are intuitive and already known, but still valuable for understanding the distribution patterns of intertidal species. Upper limits are higher moving Northwest up the coast due to lower air temperatures, larger tidal amplitude, more extreme wave environments, and more constant wetting by rain, fog, and spray. The detection of higher upper limits in the Northwest also may in part reflect a response to interannual variability, which results in particularly large-magnitude peaks in sea level in the time series in the Northwest (Figure 4). Including PC2 and its component variables within the models allowed us to account for variation contributed by other variables that influence vertical distribution that are associated with geographic location - namely slope, aspect, and wave environment - for which data are simply not available at so many field sites. Our ability to account for variation associated with geography in our model through the inclusion of these terms speaks to the strength of the MARINe program's site selection methods. The CBS samples the entire rocky intertidal zone with the same methodology across sites, and plot locations were carefully selected to minimize variation associated with differences in habitat availability among sites. In a general sense, MARINe selects sites that are comparable in their habitat availability by having contiguous rocky benches spanning the entire tidal range that also have rocky habitat above the sampled extent (i.e., above the upper limit of marine biology at the site). The relationship between slope, aspect, and vertical distribution would be driven by the interaction between those features and the local wave climate, and this type of information is not available at most of the sites. By eliminating variation in sampling design, effort, and expertise, CBS survey data can address questions

related to biogeography and species shifts at the scale of the entire coastline.

The lack of a significant correlation between our other predictor variables (residuals (d) and preceding year residual mean (d̄)) and upper limits for most taxa suggest that intertidal taxa largely may not respond to short-term sea-level variability. Still, the inclusion of these variables in our model essentially as nuisance variables allowed us to account for regular short-term variation. A negative correlation was found between upper limits of four taxa and residuals, but regardless, a positive correlation with lunar declination and long-term sea-level trend was also found. No significant correlations were found for the other taxa, which are generally longer lived and would not be expected to respond to short-term variability as readily.

4.5 | Potential Ecological Consequences

Shifts in the vertical distribution of taxa modeled here may have ecosystem level effects. *Mytilus californianus* is known to dominate benthic space in the middle intertidal zone across the NPC and modify patterns of biodiversity through both outcompeting other species for space and harboring high levels of infaunal diversity (Paine 1966, 1969, 1974; Ricketts and Calvin 1939; Suchanek 1992). Although mussel bed distribution may be modified by short-term stressors such as extreme wave events, long-term studies suggest boundaries remain somewhat constant though time (Paine 1974; Paine and Levin 1981). Any shift in the distribution of *M. californianus* will have significant impacts on the rest of the community. Studies have documented long-term declines in abundance of *M. californianus* populations in much of southern California believed to be associated with increasing sea-surface temperatures and changing upwelling regimes (Smith, Fong, and Ambrose 2006b), and climate change may be leading to declines in mussel bed infaunal diversity across much of California (Smith, Fong, and Ambrose 2006a). Further stress to this species because of accelerating SLR may have significant ecosystem level effects. *Endocladia muricata* is one of the most common algae in the upper intertidal zone in much of California, sheltering a high diversity of infaunal organisms (Glynn 1965), and facilitating recruitment of species such as *M. californianus* in its lower range and *S. compressa* in its upper range (Johnson and Brawley 1998; Readdie 2004). *Fucus* spp. forms dense canopies in the middle and upper intertidal zones and play an important role in limiting desiccation stress to other species, and individual adults are believed to live between 2 and 5 years, depending on wave exposure (Pacific Rocky Intertidal Monitoring: Target Species n.d.). *Balanus glandula* forms dense bands in the upper intertidal zone where few other invertebrates and algae are present, and adults can live longer than 10 years. It is also known to facilitate the recruitment of *E. muricata* through reducing limpet grazing (Farrell 1991; Readdie 2004). Because of their significant ecological roles, shifts in the distribution of these taxa may have widespread ecosystems impacts.

Inherent differences in life history (such as the life expectancy of sessile adults) and mobility of these organisms may cause shifting competitive hierarchies as they move upward on the

shore, which can result in changes in the relative abundance of foundation species and their associated epibionts. Previous work suggests that recruitment to upper shore levels, which would be required to allow intertidal populations to shift their distributions upward in response to SLR, requires the presence of a facilitator (Johnson and Brawley 1998; Readdie 2004). Our research further informs how SLR might impact the intertidal zone of the NPC through a combination of shifting environmental conditions across the landscape and successional, habitat cascade processes. In the upper intertidal zone, the annual recruitment and shorter adult life expectancy of *B. glandula* and *Fucus* spp. may allow them to shift more readily to short-term pulses of sea level. The upward shift in *B. glandula* could facilitate the recruitment of *E. muricata* to higher levels, which in turn could facilitate the movement of *S. compressa* and *M. californianus*.

4.6 | General Conclusions and Future Directions

An upward shift does not necessarily pose a threat to intertidal species if rocky substrate is available at higher elevations for species to colonize. But if intertidal reefs are backed by steep cliffs, soft sediments, or anthropogenic structures, and the magnitude of SLR is substantial, species may experience coastal squeeze as sea-level rise, leading to substantial habitat loss (Doody 2013; Hollenbeck, Olsen, and Haig 2014; Jackson and Mcilvenny 2011; Kaplanis et al. 2020; Schaefer et al. 2020; Vaselli et al. 2008). As habitat area is compressed, biotic interactions structuring this system will change. Increased competition for space may cause declines in abundance, biodiversity, and community net production, changes which pose considerable conservation challenges for these species (Kaplanis et al. 2020; Rilov et al. 2021; Vaselli et al. 2008).

Continued monitoring of these populations by MARINe and others will allow tracking of these shifts and determination of subsequent ecosystem impacts of SLR. Our ability to detect changes in vertical distribution may be limited by the temporal extent and resolution of data, in comparison with the temporal scales over which vertical distribution shifts occur, but investing in further monitoring can provide crucial data for understanding global change impacts (Kaplanis 2023). Although upper limits may be shifting on average in response to the long-term trends, our results suggest that cyclical forcing at multiple temporal scales (from seasonal to multi-decadal) is also important. Through changing emersion time, cyclical variation in lunar declination drives changes in vertical distribution on its own, but it may also cause alternating periods of susceptibility or buffering to global change associated extreme events such as storms or aerial heat waves (Burnaford, Nielsen, and Williams 2014; Harley, Helmuth, and Carolina 2003; Helmuth et al. 2006; Hesketh and Harley 2023). Our results can help researchers and managers interpret the impacts of these extreme events, which may have more pronounced impacts than gradual changes in average environmental conditions (Denny et al. 2009; Gaines and Denny 1993; Hawkins, Burrows, and Mieszkowska 2023; Hesketh and Harley 2023; Mieszkowska et al. 2021; Mislan, Wethey, and Helmuth 2009; Raymond et al. 2022; Wethey et al. 2011). Continued sampling over a long temporal extent will be crucial to disentangling the effects of natural variation in environmental drivers from those associated with anthropogenic global climate change.

Although the results found here are broadly applicable, the relative influence of the long-term drivers of vertical distribution discussed here vary across locations that experience different tidal regimes and rates of SLR, and this remains an understudied area of research (Haigh, Eliot, and Pattiaratchi 2011; Menéndez and Woodworth 2010). Few studies have documented long-term impacts of SLR on rocky intertidal organisms, as the data required to address this question are difficult to obtain. Multiple studies have documented impacts linked to the 18.6-year cycle of lunar declination on the NPC, but we were not able to find studies evaluating the impact of this cycle in other locations (Burnaford, Nielsen, and Williams 2014; Denny and Paine 1998; Harley and Paine 2009). In locations with mixed and diurnal tides, the 18.6-year cycle significantly modifies tidal amplitude, but the magnitude of variation within and across these regions is spatially variable (Figure 5) (Haigh, Eliot, and Pattiaratchi 2011; Menéndez and Woodworth 2010). In addition, perigean (4.4-year) cycles can also cause significant variation in tidal amplitude, sometimes exceeding that caused by the 18.6-year cycle, especially in areas with semidiurnal tides (Haigh, Eliot, and Pattiaratchi 2011; Menéndez and Woodworth 2010). In locations with large amplitude tides, such as the sea of Okhotsk, New England, Newfoundland, and northern Europe, variation in tidal amplitude associated with both the 18.6 and 4.4-year cycles is greater than that observed on the NPC (Haigh, Eliot, and Pattiaratchi 2011; Menéndez and Woodworth 2010). Fortunately, excellent, large-scale long-term monitoring programs exist in regions around the globe that now provide multidecadal, large-scale data comparable to those used here, from which future studies can determine the relative influence of short and long-term drivers on vertical distribution of intertidal organisms (Coletti et al. 2016; Gilbane et al. 2022; Hawkins, Burrows, and Mieszkowska 2023; Kaplanis 2023; Mieszkowska et al. 2014).

Author Contributions

Nikolas J. Kaplanis: conceptualization, data curation, formal analysis, funding acquisition, investigation, methodology, project administration, resources, software, supervision, validation, visualization, writing – original draft, writing – review and editing. **Mark W. Denny:** conceptualization, data curation, formal analysis, investigation, methodology, writing – review and editing. **Peter T. Raimondi:** conceptualization, data curation, formal analysis, funding acquisition, investigation, methodology, project administration, resources, supervision, validation, visualization, writing – review and editing.

Conflicts of Interest

The authors declare no conflicts of interest.

Data Availability Statement

The data and code that support the findings of this study are openly available in Zenodo at https://doi.org/10.5281/zenodo.11186904.

References

Burnaford, J. L., K. J. Nielsen, and S. L. Williams. 2014. "Celestial Mechanics Affects Emersion Time and Cover Patterns of an Ecosystem Engineer, the Intertidal Kelp *Saccharina sessilis*." *Marine Ecology Progress Series* 509: 127–136. https://doi.org/10.3354/meps10876.

Cazenave, A., H. Dieng, B. Meyssignac, K. Von Schuckmann, B. Decharme, and E. Berthier. 2014. "The Rate of Sea-Level Rise." *Nature Climate Change* 4, no. May: 358–361. https://doi.org/10.1038/NCLIMATE2159.

Chelton, D. B., and R. E. Davis. 1982. "Monthly Mean Sea-Level Variability Along the West Coast of North America." *Journal of Physical Oceanography* 12: 757–784.

Chen, X., X. Zhang, J. A. Church, et al. 2017. "The Increasing Rate of Global Mean Sea-Level Rise During 1993–2014." *Nature Climate Change* 7, no. July: 492–495. https://doi.org/10.1038/NCLIMATE3325.

Church, J. A., P. U. Clark, A. Cazenave, et al. 2013. "Sea Level Change." In *Climate Change 2013: The Physical Science Basis. Contribution of Working Group I to the Fifth Assessment Report of the Intergovernmental Panel on Climate Change*, edited by T. F. Stocker, D. Qin, G.-K. Plattner, M. Tignor, S. K. Allen, J. Boschung, A. Nauels, Y. Xia, V. Bex, and P. M. Midgley. Cambridge, UK and New York, NY, USA: Cambridge University Press.

Church, J. A., and N. J. White. 2006. "A 20th Century Acceleration in Global Sea-Level Rise." *Geophysical Research Letters* 33: 94–97. https://doi.org/10.1029/2005GL024826.

Coletti, H. A., J. L. Bodkin, D. H. Monson, B. E. Ballachey, and T. A. Dean. 2016. "Detecting and Inferring Cause of Change in an Alaska Nearshore Marine Ecosystem." *Ecosphere* 7, no. October: 1–20.

Connell, J. H. 1961. "The Influence of Interspecific Competition and Other Factors on the Distribution of the Barnacle *Chthalamus stellatus*." *Ecology* 42, no. 4: 710–723.

Connell, J. H. 1972. "Interactions on Marine Rocky Intertidal Shores." *Annual Review of Ecology and Systematics* 3, no. 22: 169–192. https://doi.org/10.1146/annurev.es.03.110172.001125.

Dayton, P. K. 1971. "Competition, Disturbance, and Community Organization: The Provision and Subsequent Utilization of Space in a Rocky Intertidal Community." *Ecological Monographs* 41, no. 4: 351–389. https://doi.org/10.1146/annurev.ecolsys.33.010802.150515.

Denny, M. W., B. Helmuth, G. H. Leonard, C. D. G. Harley, L. J. H. Hunt, and E. K. Nelson. 2004. "Quantifying Scale in Ecology: Lessons From a Wave-Swept Shore." *Ecological Monographs* 74, no. 3: 513–532.

Denny, M. W., L. J. H. Hunt, L. P. Miller, and C. D. G. Harley. 2009. "On the Prediction of Extreme Ecological Events." *Ecological Monographs* 79, no. 3: 397–421. https://doi.org/10.1890/08-0579.1.

Denny, M. W., and R. T. Paine. 1998. "Celestial Mechanics, Sea Level Changes, and Intertidal Ecology." *Biological Bulletin* 194, no. 18: 108–115. https://doi.org/10.2307/1543040.

Doody, J. P. 2013. "Coastal Squeeze and Managed Realignment in Southeast England, Does It Tell Us Anything About the Future?" *Ocean and Coastal Management* 79: 34–41. https://doi.org/10.1016/j.ocecoaman.2012.05.008.

Doty, M. S. 1946. "Critical Tide Factors That Are Correlated With the Vertical Distribution of Marine Algae and Other Organisms Along the Pacific Coast." *Ecology* 27, no. 4: 315–328.

Enfield, D. B., and J. S. Allen. 1979. "On the Structure and Dynamics of Monthly Mean Sea Level Anomalies Along the Pacific Coast of North and South America." *Journal of Physical Oceanography* 10: 557–578.

Farrell, T. M. 1991. "Models and Mechanisms of Succession: An Example From a Rocky Intertidal Community." *Ecological Monographs* 61, no. 1: 95–113.

Gaines, S., and J. Roughgarden. 1985. "Larval Settlement Rate: A Leading Determinant of Structure in an Ecological Community of the Marine Intertidal Zone." *Proceedings of the National Academy of Sciences of the United States of America* 82, no. 11: 3707–3711.

Gaines, S. D., and M. W. Denny. 1993. "The Largest, Smallest, Highest, Lowest, Longest, and Shortest: Extremes in Ecology." *Ecology* 74, no. 6: 1677–1692.

Gilbane, L., R. F. Ambrose, J. L. Burnaford, et al. 2022. "Long-Term Sustainability of Ecological Monitoring: Perspectives From the Multi-Agency Rocky Intertidal Network." In *Partnerships in Marine Research*, 109–129. Netherlands: Elsevier Inc. https://doi.org/10.1016/b978-0-323-90427-8.00007-1.

Glynn, P. W. 1965. "Community Composition, Structure, and Interrelationships in the Marine Intertidal Endocladia Muricata—Balanus Glandula Association in Monterey Bay, California." *Beaufortia* 12, no. 148: 4–198.

Graham, M. H., P. K. Dayton, and J. M. Erlandson. 2003. "Ice ages and Ecological Transitions on Temperate Coasts." *Trends in Ecology & Evolution* 18, no. 1: 33–40.

Haigh, I. D., M. Eliot, and C. Pattiaratchi. 2011. "Global Influences of the 18.61 Year Nodal Cycle and 8.85 Year Cycle of Lunar Perigee on High Tidal Levels." *Journal of Geophysical Research: Oceans* 116, no. 6: 1–16. https://doi.org/10.1029/2010JC006645.

Harley, C. D. G., B. S. T. Helmuth, and S. Carolina. 2003. "Local- and Regional-Scale Effects of Wave Exposure, Thermal Stress, and Absolute Versus Effective Shore Level on Patterns of Intertidal Zonation." *Limnology and Oceanography* 48, no. 4: 1498–1508.

Harley, C. D. G., R. A. Hughes, K. M. Hultgren, et al. 2006. "The Impacts of Climate Change in Coastal Marine Systems." *Ecology Letters* 9, no. 2: 228–241. https://doi.org/10.1111/j.1461-0248.2005.00871.x.

Harley, C. D. G., and R. T. Paine. 2009. "Contingencies and compounded rare perturbations dictate sudden distributional shifts during periods of gradual climate change." *Proceedings of the National Academy of Sciences of the United States of America* 106: 11172–11176. www.pnas.org/cgi/content/full/.

Hawkins, S. J., M. T. Burrows, and N. Mieszkowska. 2023. "Shoreline Sentinels of Global Change Show the Consequences of Extreme Events." *Global Change Biology* 29, no. 1: 7–9. https://doi.org/10.1111/gcb.16477.

Helmuth, B., B. R. Broitman, C. A. Blanchette, et al. 2006. "Mosaic Patterns of Thermal Stress in the Rocky Intertidal Zone: Implications for Climate Change." *Ecological Monographs* 76, no. 4: 461–479. https://doi.org/10.1890/0012-9615(2006)076[0461:MPOTSI]2.0.CO;2.

Hesketh, A. V., and C. D. G. Harley. 2023. "Extreme Heatwave Drives Topography-Dependent Patterns of Mortality in a Bed-Forming Intertidal Barnacle, With Implications for Associated Community Structure." *Global Change Biology* 29, no. 1: 165–178. https://doi.org/10.1111/gcb.16390.

Hollenbeck, J. P., M. J. Olsen, and S. M. Haig. 2014. "Using Terrestrial Laser Scanning to Support Ecological Research in the Rocky Intertidal Zone." *Journal of Coastal Conservation* 18, no. 6: 701–714. https://doi.org/10.1007/s11852-014-0346-8.

Hughes, B. B., R. Beas-Luna, A. K. Barner, et al. 2017. "Long-Term Studies Contribute Disproportionately to Ecology and Policy." *BioScience* 67, no. 3: 271–278. https://doi.org/10.1093/biosci/biw185.

Hunt, L. J. H. 2006. *The Rise of Endocladia Muricata: Punctuated Change At An Abrupt Range Edge [Dissertation]*. Stanford, CA: Stanford University.

Jackson, A. C., and J. Mcilvenny. 2011. "Coastal Squeeze on Rocky Shores in Northern Scotland and Some Possible Ecological Impacts." *Journal of Experimental Marine Biology and Ecology* 400, no. 1–2: 314–321. https://doi.org/10.1016/j.jembe.2011.02.012.

Johnson, L. E., and S. H. Brawley. 1998. "Dispersal and Recruitment of a Canopy-Forming Intertidal Alga: The Relative Roles of Propagule Availability and Post-Settlement Processes." *Oecologia* 117: 517–526.

Kaplanis, N. J. 2023. "Insight Into Best Practices: A Review of Long-Term Monitoring of the Rocky Intertidal Zone of the Northeast Pacific Coast." *Frontiers in Marine Science* 10: 1–20. https://doi.org/10.3389/fmars.2023.1182562.

Kaplanis, N. J. 2024. "Data and Analysis for Kaplanis, Denny, and Raimondi 2024, 'Vertical Distribution of Rocky Intertidal Organisms Shifts With Sea-Level Variability on the Northeast Pacific Coast'." https://doi.org/10.5281/zenodo.11186904.

Kaplanis, N. J., C. B. Edwards, Y. Eynaud, and J. E. Smith. 2020. "Future Sea-Level Rise Drives Rocky Intertidal Habitat Loss and Benthic Community Change." *PeerJ* 8: e9186. https://doi.org/10.7717/peerj.9186.

Kaplanis, N. J., C. B. Edwards, Y. Eynaud, and J. E. Smith. 2020. "Future Sea-Level Rise Drives Rocky Intertidal Habitat Loss and Benthic Community Change." *PeerJ* 8: e9186. https://doi.org/10.7717/peerj.9186.

Lewis, J. R. 1964. *The Ecology of Rocky Shores* (W. S. Bullough, Ed.). London: English Universities Press Ltd.

Lindenmayer, D. B., E. L. Burns, P. Tennant, et al. 2015. "Contemplating the Future: Acting Now on Long-Term Monitoring to Answer 2050's Questions." *Austral Ecology* 40, no. 3: 213–224. https://doi.org/10.1111/aec.12207.

Lindenmayer, D. B., G. E. Likens, A. Andersen, et al. 2012. "Value of Long-Term Ecological Studies." *Austral Ecology* 37, no. 7: 745–757. https://doi.org/10.1111/j.1442-9993.2011.02351.x.

Littler, M. M., and D. S. Littler. 1987. "Effects of Stochastic Processes on Rocky-Intertidal Biotas: An Unusual Flash Flood Near Corona del Mar, California." *Bulletin of the Southern California Academy of Sciences* 86, no. 2: 95–106.

Menéndez, M., and P. L. Woodworth. 2010. "Changes in Extreme High Water Levels Based on a Quasi-Global Tide-Gauge Data Set." *Journal of Geophysical Research: Oceans* 115, no. 10: 1–15. https://doi.org/10.1029/2009JC005997.

Menge, B. A. 1976. "Organization of the New England Rocky Intertidal Community: Role of Predation, Competition, and Environmental Heterogeneity." *Ecological Monographs* 46, no. 4: 355–393. https://doi.org/10.2307/1942563.

Menge, B. A. 1995. "Indirect Effects in Marine Rocky Intertidal Interaction Webs: Patterns and Importance." *Ecological Monographs* 65, no. 1: 21–74.

Menge, B., F. Chan, and J. Lubchenco. 2008. "Response of a Rocky Intertidal Ecosystem Engineer and Community Dominant to Climate Change." *Ecology Letters* 11: 151–162. https://doi.org/10.1111/j.1461-0248.2007.01135.x.

Mieszkowska, N., M. T. Burrows, S. J. Hawkins, and H. Sugden. 2021. "Impacts of Pervasive Climate Change and Extreme Events on Rocky Intertidal Communities: Evidence From Long-Term Data." *Frontiers in Marine Science* 8: 1–17. https://doi.org/10.3389/fmars.2021.642764.

Mieszkowska, N., H. Sugden, L. B. Firth, and S. J. Hawkins. 2014. "The Role of Sustained Observations in Tracking Impacts of Environmental Change on Marine Biodiversity and Ecosystems." *Philosophical Transactions of the Royal Society A* 372: 1–13. https://doi.org/10.1098/rsta.2013.0339.

Mislan, K. A. S., D. S. Wethey, and B. Helmuth. 2009. "When to Worry About the Weather: Role of Tidal Cycle in Determining Patterns of Risk in Intertidal Ecosystems." *Global Change Biology* 15, no. 12: 3056–3065. https://doi.org/10.1111/j.1365-2486.2009.01936.x.

Multi-Agency Rocky Intertidal Network (MARINe) Survey Methods. n.d. https://marine.ucsc.edu/methods/index.html.

National Research Council. 2012. *Sea-Level Rise for the Coasts of California, Oregon, and Washington: Past, Present, and Future.* Washington D.C.: National Academies Press. https://doi.org/10.17226/13389.

NOAA. 2001. "Tidal Datums and Their Applications." https://tidesandcurrents.noaa.gov/publications/tidal_datums_and_their_applications.pdf.

NOAA Tides and Currents, Relative Sea Level Trends. n.d. https://tidesandcurrents.noaa.gov/sltrends/sltrends.html.

NOAA's Vertical Datum Transformation Tool (VDatum v. 4.7) (4.7). n.d. "National Oceanic and Atmospheric Administration (NOAA) National Geodetic Survey (NGS), Office of Coast Survey (OCS), and Center for Oceanographic Products and Services (CO-OPS)." Accessed August 29, 2024. https://vdatum.noaa.gov/.

Pacific Rocky Intertidal Monitoring: Target Species. n.d. http://www.eeb.ucsc.edu/pacificrockyintertidal/target/index.html.

Paine, R. T. 1966. "Food Web Complexity and Species Diversity." *American Naturalist* 100, no. 910: 65–75.

Paine, R. T. 1969. "A Note on Trophic Complexity and Community Stability." *American Naturalist* 103, no. 929: 91–93. https://doi.org/10.1086/282586.

Paine, R. T. 1974. "Intertidal Community Structure. Experimental Studies on the Relationship Between a Dominant Competitor and Its Principal Predator." *Oecologia* 15, no. 2: 93–120.

Paine, R. T. 1980. "Food Webs: Linkage, Interaction Strength and Community Infrastructure." *Journal of Animal Ecology* 49, no. 3: 666–685.

Paine, R. T., and S. A. Levin. 1981. "Intertidal Landscapes: Disturbance and the Dynamics of Pattern." *Ecological Monographs* 51, no. 2: 145–178.

R Core Team. 2021. *R: A Language and Environment for Statistical Computing.* Vienna, Austria: R Foundation for Statistical Computing. https://www.r-project.org/.

Rahmstorf, S. 2010. "A New View on Sea Level Rise." *Nature Reports Climate Change* 4, no. April: 1. https://doi.org/10.1029/2010GL042947.

Raymond, W. W., J. S. Barber, M. N. Dethier, et al. 2022. "Assessment of the Impacts of an Unprecedented Heatwave on Intertidal Shellfish of the Salish Sea." *Ecology* 103, no. 10: 1–7. https://doi.org/10.1002/ecy.3798.

Readdie, M. D. 2004. *Facilitation in the Rocky Intertidal and Its Effects on Vertical Zonation.* Santa Cruz: University of California.

Ricketts, E. F., and J. Calvin. 1939. *Between Pacific Tides* (J. W. Hedgpeth, Ed.). 1st ed. Stanford: Stanford University Press.

Rilov, G., N. David, T. Guy-Haim, D. Golomb, R. Arav, and S. Filin. 2021. "Sea Level Rise Can Severely Reduce Biodiversity and Community Net Production on Rocky Shores." *Science of the Total Environment* 791: 148377. https://doi.org/10.1016/j.scitotenv.2021.148377.

Roughgarden, J., S. Gaines, and H. Possingham. 1988. "Recruitment Dynamics in Complex Life Cycles." *Science* 241, no. 4872: 1460–1466. https://doi.org/10.1126/science.11538249.

Schaefer, N., M. Mayer-Pinto, K. J. Griffin, E. L. Johnston, W. Glamore, and K. A. Dafforn. 2020. "Predicting the Impact of Sea-Level Rise on Intertidal Rocky Shores With Remote Sensing." *Journal of Environmental Management* 261, no. 110203: 1–9. https://doi.org/10.1016/j.jenvman.2020.110203.

Smith, J. R., P. Fong, and R. F. Ambrose. 2006a. "Dramatic Declines in Mussel Bed Community Diversity: Response to Climate Change?" *Ecology* 87, no. 5: 1153–1161. https://doi.org/10.1890/0012-9658(2006)87[1153:DDIMBC]2.0.CO;2.

RIGHTS LINK()

Smith, J. R., P. Fong, and R. F. Ambrose. 2006b. "Long-Term Change in Mussel (*Mytilus californianus* Conrad) Populations Along the Wave-Exposed Coast of Southern California." *Marine Biology* 149, no. 3: 537–545. https://doi.org/10.1007/s00227-005-0223-y.

Stickle, W. B., M. Lindeberg, S. D. Rice, K. Munley, and V. Reed. 2016. "Seasonal Changes in the Thermal Regime and Gastropod Tolerance to Temperature and Desiccation Stress in the Rocky Intertidal Zone in Southeast Alaska." *Journal of Experimental Marine Biology and Ecology* 482: 56–63. https://doi.org/10.1016/j.jembe.2016.04.011.

Stommel, H. 1963. "Varieties of Oceanographic Experience." *Science* 139, no. 3555: 572–576.

Suchanek, T. H. 1992. "Extreme Biodiversity in the Marine Environment: Mussel Bed Communities of *Mytilus californianus*." *Northwest Environmental Journal* 8: 150. https://cir.nii.ac.jp/crid/1370848655021877633.bib?lang=en.

Sweet, W., J. Park, C. Zervas, and S. Gill. 2014. "Sea Level Rise and Nuisance Flood Frequency Changes Around the United States." NOAA Technical Report NOS CO-OPS 073.

Sweet, W. V., R. E. Kopp, C. P. Weaver, et al. 2017. "Global and Regional Sea Level Rise Scenarios for the United States." NOAA Technical Report NOS CO-OPS 083.

Thorner, J., L. Kumar, and S. D. A. Smith. 2014. "Impacts of Climate-Change-Driven Sea Level Rise on Intertidal Rocky Reef Habitats Will Be Variable and Site Specific." *PLoS One* 9, no. 1: 1–7. https://doi.org/10.1371/journal.pone.0086130.

Toms, J. A., J. S. Compton, M. Smale, and S. von der Heyden. 2014. "Variation in Palaeo-Shorelines Explains Contemporary Population Genetic Patterns of Rocky Shore Species." *Biology Letters* 10, no. 6: 20140330. https://doi.org/10.1098/rsbl.2014.0330.

Underwood, A. J. 1980. "The Effects of Grazing by Gastropods and Physical Factors on the Upper Limits of Distribution of Intertidal Macroalgae." *Oecologia (Berl.)* 46: 201–213.

Underwood, A. J., and P. Jernakoff. 1984. "The Effects of Tidal Height, Wave-Exposure, Seasonality And Rock-Pools On Grazing And the Distribution Of Intertidal Macroalgae In New South Wales." *Journal of Experimental Marine Biology and Ecology* 75: 71–96.

Valentine, J. W., and D. Jablonski. 1991. "Biotic Effects of Sea Level Changes." *Journal of Geophysical Research* 96, no. 90: 6873–6878.

Vaselli, S., I. Bertocci, E. Maggi, and L. Benedetti-Cecchi. 2008. "Assessing the Consequences of Sea Level Rise: Effects of Changes in the Slope of the Substratum on Sessile Assemblages of Rocky Seashores." *Marine Ecology Progress Series* 368: 9–22. https://doi.org/10.3354/meps07625.

Wethey, D. S., S. A. Woodin, T. J. Hilbish, S. J. Jones, F. P. Lima, and P. M. Brannock. 2011. "Response of Intertidal Populations to Climate: Effects of Extreme Events Versus Long Term Change." *Journal of Experimental Marine Biology and Ecology* 400, no. 1–2: 132–144. https://doi.org/10.1016/j.jembe.2011.02.008.

Supporting Information

Additional supporting information can be found online in the Supporting Information section.